Open Access Research Journal of
Engineering and Technology
Journals home page: https://oarjpublication/journals/oarjet/
ISSN: 2783-0128 (Online)

(REVIEW ARTICLE)

Advancements in metal organic frameworks for energy storage applications: A review of current research and future directions

Samin Yeasar Zahan Sparsha [1,*], Usoshi Mohsin [2], Olakunle Ibrahim Oresegun [3], Reuben Zakari Kabantiyok [4] Sekete Maseala Camilla [5] and Okeoma Kingsley Emeka [6]

[1] *Department of Physics and Astronomy, East Texas A&M University, Commerce, Texas, USA.*
[2] *Department of Chemistry, East Texas A&M University, Commerce, Texas, USA.*
[3] *Department of Mechanical Engineering, Zhejiang University, Hangzhou, China.*
[4] *Department of Research and Innovation, Schrödinger Technologies, Kano State, Nigeria.*
[5] *Department of Industrial Design Engineering, Zhejiang University, Hangzhou, China.*
[6] *Department of Inspection Control, Hydrodive Limited, Lagos, Nigeria.*

Open Access Research Journal of Engineering and Technology, 2025, 09(02), 007-031

Publication history: Received on 25 September 2025; revised on 08 November 2025; accepted on 10 November 2025

Article DOI: https://doi.org/10.53022/oarjet.2025.9.2.0088

Abstract

The increasing energy needs globally with pressing environmental requirements necessitate the discovery of new energy storage technologies. Metal-Organic Frameworks (MOFs) have emerged as a revolutionary class of porous materials with superior structural tunability, high surface area, and porosity and are leading candidates for next-generation energy applications. In this review, an overview of the recent advances in MOF-based materials as utilized in different energy storage technologies is presented. We review the multifunctional applications of MOFs and their derivatives as electrode materials in various batteries, including lithium-ion, sodium-ion, lithium-sulfur and zinc batteries, and high-performance supercapacitors. Their crucial application for hydrogen storage, as well as their computational and AI-driven approach, is also discussed. A critical analysis of the current challenges, including low electronic conductivity and structural instability, is presented alongside a description of promising future directions, such as the use of MOF-derived composites, hybrid architectures, and the integration of computational design methods. Overall, this review highlights the significant promise of MOFs for transforming the landscape of sustainable energy technology.

Keywords: Metal-Organic Frameworks (MOFS); Energy Storage; Electrode Materials; Hydrogen Storage; Computational Design

1. Introduction

The global need for energy is fast increasing, but it must also deal with serious environmental pollution concerns and decreasing resources. [1]. To address these critical concerns, a great number of research efforts have been established and carried out. Global demand for energy resources has regularly and significantly increased in recent years, prompting considerable worries about the long-term viability of fuel supply and environmental difficulties such as climate change, melting glaciers, and rising sea levels [2]. Renewable, safe, clean, and sustainable energy storage and conversion technologies have emerged as an increasingly significant research topic. To address the energy crisis and environmental issues, efficient and sustainable energy storage and conversion technologies must be developed. [3, 4]. Metal-Organic Frameworks (MOFs) have emerged as a transformational class of materials, providing a compelling alternative to traditional technologies in a variety of energy conversion and storage devices [5-7]. This paper thoroughly covers advances in MOFs for energy storage, stressing their distinguishing characteristics, numerous uses, and the hurdles that must be overcome before they can be widely used.

* Corresponding author: Samin Yeasar Zahan Sparsha

Copyright © 2025 Author(s) retain the copyright of this article. This article is published under the terms of the Creative Commons Attribution License 4.0.

Metal-Organic Frameworks are a rapidly growing class of crystalline porous materials [8]. Their essential structure is generated by the exact self-assembly of inorganic metal ions or clusters, called as Secondary Building Units (SBUs), and organic ligands, or linkers, joined by strong coordination connections [9]. This self-assembly process produces topologically varied and well-defined structures that extend in one, two, or three dimensions, with organized, extremely porous networks [10] (Figure 1a). MOFs are formally categorized as a subclass of coordination networks, which lie within the larger category of coordination polymers [11, 12]. They feature a variety of tunable qualities, including as structural tuneability, high porosity, a large specific surface area, and better conductivity, as shown in Figure 1b [13].

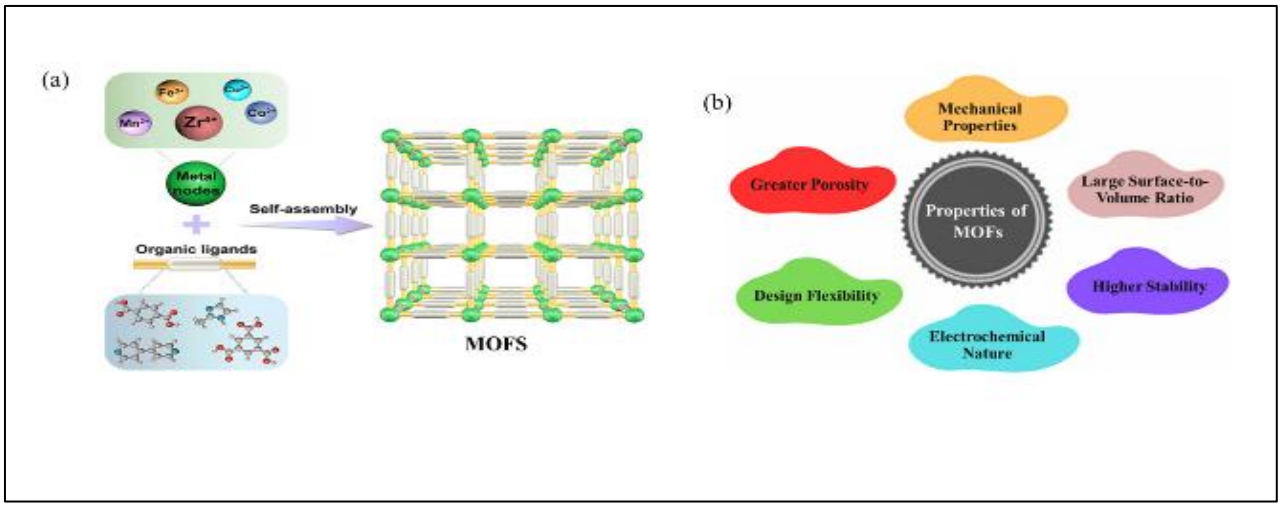

Figure 1 Schematic Illustration of Self-Assembly of MOFs [14] (b) Distinguishing properties of MOFs [13]

The pioneering research on MOF-5, consisting of zinc oxide clusters and terephthalate linkers, put the focus on the potentiality of MOFs by demonstrating them to be endowed with exceptional attributes such as high surface area, structural stability, and exceptional versatility. The early discovery unlocked MOFs as a versatile platform technology [15]. The innate ability to design the metal and organic building block components allows for the incorporation of functionalities of interest, e.g., electroactive sites such as redox-active metal centers, directly influencing the performance of the material [16, 17]. Such precise control over their composition, structural characteristics, and tunable porosities renders MOFs extremely attractive to be used in a multitude of applications ranging from drug delivery, gas adsorption, separation, catalysis, sensing, to most significantly, energy storage and conversion [18]. The modular nature of MOF construction, with attributes resembling a molecular "LEGO" system, provides unprecedented control over their structural, chemical, and physical properties at the molecular level [19]. It is this very rational and foreseeable design methodology that allows materials to be designed with specific performance characteristics specifically for particular energy storage applications, thus accelerating the shift from basic research to practical application [20].

So far, several synthetic methodologies for MOF preparation have been investigated, including solvothermal reactions [21], hydrothermal methods [21], electrochemical routes [22], mechanochemical methods [23], and microwave irradiation methods [24]. Table 1 compares the methods of synthesizing MOFs. Among these, the solvothermal synthesis technique is a simple and widely used method for producing well-defined MOFs at moderate temperatures (below 3000C) [25]. It is essential to accurately control experimental conditions, such as reaction temperature, the selections of the appropriate functional linkers and metal sources, the concentrations of metal salt and ligand, and the pH of the solution for adjusting chemical components, surface morphology, pore sizes, and microstructure of MOFs during the solvothermal process [26]. To adjust chemical components, surface morphology, pore sizes, and microstructure of MOFs during the solvothermal process, it is critical to precisely control experimental conditions such as reaction temperature, the selection of appropriate functional linkers and metal sources, metal salt and ligand concentrations, and solution pH [27, 28].

Table 1 Comparison of MOF Synthesis Methods

Synthesis Method	Key Characteristics	Advantages	Limitations	Ref
Solvothermal/ Hydrothermal	Electrical heating in sealed vessels (60-300°C, high pressure); long reaction times (hours to days)	Produces high-quality single crystals for structural analysis; stable for carboxylate linkers	Small scale; long reaction times; low space-time yields; challenges for industrial scale-up; often uses expensive organic solvents	[29, 30]
Microwave-Irradiation	Rapid, uniform heating via microwave irradiation; short reaction times (minutes to hours)	Fast crystallization and nucleation; phase selectivity; narrow particle size distribution; facile morphology control; improved MOF properties (stability, conductivity, porosity); reduced/avoided toxic solvents	Potential for reduced crystal quality if conditions are not optimal	[31]
Electrochemical	Anodic dissolution of bulk metal plates to supply metal ions; ambient conditions	Simple, easy, and faster synthesis; eliminates metal salts; high linker utilization (Faraday efficiencies); continuous process potential	Rarely reported method for synthesis of MOFs.	[32, 33]
Mechanochemical	Grinding/milling (ball milling) with little/no solvent; room temperature	"Green" (solvent-free); quantitative yields; short reaction times (10-60 min); uses metal oxides (water as byproduct); can accelerate reactions (LAG/ILAG)	Limited understanding of mechanisms; difficult to obtain large product quantities; limited to specific MOF types	[34]

1.1. Importance of MOFs in Energy Storage

The worldwide demand for effective and clean energy storage and conversion has spearheaded the search for novel materials that may maximize the efficiency of electrochemical devices such as fuel cells, solar cells, supercapacitors, and batteries [35]. MOFs have emerged as a viable and efficient alternative to many conventional materials already utilized in these critical technologies [36].

The relevance of MOFs to energy storage is in their inherent structural characteristics and tunable properties [37]. Their remarkably large surface areas and porosity are of maximum importance, as these features directly affect greater energy density, longer life cycle, and enhanced stability when MOFs are applied as electrode materials or other active entities in energy storage devices [18]. The porous nature of MOFs enables facile electrolyte penetration and efficient ion transport, which is needed in the case of high-performance electrochemical devices [38]. In addition to this, MOFs present a high density of evenly distributed active sites and well-defined pore topologies, which collectively promote fast transport of electrolyte ions, dealing directly with the infamous kinetic slowness in traditional materials [16]. Apart from electrochemical applications, the vast surface area and porosity of MOFs significantly enhance the adsorption and storage of gases like hydrogen and methane, which are essential for applications like fuel cells and natural gas vehicles, with consequent enhanced energy density and overall efficiency [39].

MOFs exhibit superior design versatility, enabling one to achieve high surface-to-volume ratios and functionalization with multivalent ligands and metal centers and thus making them crucial to achieving clean and efficient energy conversion and storage. They can be used in various roles, including electrocatalytic materials, electrolyte membranes, and direct energy storage materials [40]. Their advantage lies in their ability to mitigate the limitations of conventional electrode materials: a lack of accessible sites for electrochemical reactions or slow transport of ions, which makes MOFs not just incremental new materials but truly transformative ones that can change the face of energy fundamentally [16]. Also, MOF synthesis and use are credited with causing a substantial reduction in the release of greenhouse gases compared to conventional materials, which can be explicitly observed in the development of light and high-capacity storage systems for natural gas vehicles. This environmentally friendly advantage coupled with their performance parameter makes them an ideal choice as a sustainable product in the new energy sector. The future direction of MOF application in energy storage will likely be advanced MOF-derived composites or hybrid framework systems since these

processes are able to surmount the inherent limitations of bare MOFs, e.g., low electronic conductivity and structural instability, thereby enhancing their applicability [13, 41, 42].

1.2. Scope and Objectives of the Review

This review paper aims to provide a comprehensive and critical analysis of the recent advancements in Metal-Organic Frameworks (MOFs) for diverse energy storage applications. This review is meticulously structured to provide a logical progression from fundamental concepts to advanced applications and future outlooks, ensuring a coherent and in-depth understanding of the subject matter. The review considers their use in lithium-ion, sodium-ion, and lithium-sulfur batteries, as electrodes for supercapacitors, and for efficiency in hydrogen storage. It also ventures into the new area of computer and AI-based design for MOFs, which will possibly propel material discovery and optimization ahead.

The originality of this review is its holistic and convergent approach. It not only covers the dominant energy storage applications but also links them to the larger challenges and future prospects. Unlike other reviews that may be specifically written on one application, the current paper offers a broad but inclusive view. Inclusion of a special section covering computational and AI methods for MOF synthesis also makes this work standout by highlighting a quickly emerging, state-of-the-art research frontier that is central to the practical implementation and widespread adoption of these materials. By bridging fundamental synthesis and properties with practical applications and future trends, this review forms an integrated and valuable tool for researchers.

2. Metal Organic Frameworks for Energy Storage Applications

2.1. MOFs for Battery Applications

Metal-Organic Frameworks (MOFs) and their derivatives have garnered significant interest as a class of potentially revolutionary materials for next-generation battery technologies. Their unique features like ultrahigh porosity, high specific surface area, and facile functionalization render them intriguingly promising candidates to enhance the performance of many battery systems like sodium-ion, lithium-metal, lithium-sulfur, and zinc batteries. MOFs have the potential to serve as active electrode materials, precursors to high-performance derived materials, or electrolyte and separator components that break through urgent challenges in battery construction[13].

2.2. MOFs in Lithium-Ion Batteries (LIBs)

Lithium-ion batteries (LIBs) are the most widely used and adaptable rechargeable batteries, with applications ranging from consumer electronics and industrial products to electric cars [43]. LIBs are made up of four major components: cathode and anode electrodes, a separator, and an electrolyte. The separator acts as a barrier between the anode and cathode, preventing them from coming into contact, whilst the electrolyte is an electrically conducting solution or gel that allows lithium ions to move between the anode and cathode electrodes. One of the primary goals in upgrading LIBs is to generate a high cell voltage, which can be accomplished by raising the energy difference between the redox energies of the cathode and anode. This can be accomplished by using either an anode with a higher-lying energy band that requires stabilization of lower oxidation states or cathodes with a lower-lying energy band that requires stabilization of higher oxidation states. LIBs are rechargeable batteries, therefore they have two basic processes: discharging and charging, as shown in Figures 2a and 2b, respectively.

MOFs have recently sparked widespread interest and emerged as a promising material in the sectors of energy storage and batteries. A wide range of MOFs and related materials have been used as battery components, including cathode [44] and anode [45] electrodes as well as separators [46].]. This is because MOFs have extremely large surface areas, as well as short and rapid ion diffusion paths and distances. Furthermore, MOFs have a large and adjustable porosity, which allows for a wide range of possibilities for depositing produced products while preventing electrode volume growth during charging and discharging operations [47].

Fang and colleagues developed a Co-MOF-derived 2D porous leaf-like Co3O4 nanosheet over a 3D nickel foam (Co3O4/3DNF) as a binder-free anode electrode for LIBs [48]. Co3O4/3DNF exhibits an outstanding cyclic stability for up to 2000 cycles with an ultrahigh rate capability at 25 A g-1. Co3O4/3DNF has remarkable cyclic stability for up to 2000 cycles and an ultrahigh rate capability of 25 A g-1. Co3O4 produced from MOFs has a large surface area, which increases the exposure and contact of active sites for electrochemical redox processes. Furthermore, porous leaf-like Co3O4 nanosheets buffer electrode volume expansion and reduce Li+ diffusion length during cycling. Together with the 3D nickel foam, a synergistic effect is achieved in which the composite exhibits excellent electrical conductivity, which improves the mediocre electrical conductivity of Co3O4 nanosheets [48]. When compared to conventional techniques of producing Co3O4, the porous Co3O4 material generated from MOFs exhibits advantageous features. Sun et al. [49]

found that mesoporous Co3O4 hollow spheres are cyclically stable for 7000 cycles at 5 A g1, however the material has a low specific capacity. Similarly, prior research on Co3O4 nanobelt [50] and nanowire [51] arrays indicated lower rate capability and poor cycling performance when compared to the MOF-derived Co3O4 coated on nickel foam.

Hu et al. [52] used pyrolyzed Se-doped ZIF-67 to synthesize CoSe nanoparticles encapsulated in a hollow carbon shell. The synthesised CoSe@C displayed exceptional cyclability by maintaining 91.6% discharge capacity, benefiting from the structural protection and charge transport channels provided by the hollow carbon matrix. In order to increase the theoretical capacity, Zhang et al. [53] used a newly developed MOF of Cu(2,7 AQDC) (2,7-H2AQDC = 2,7-anthraquinonedicarboxylate), which has separate redox activities at both Cu2(Ac)4 nodes and anthraquinone ligands. This resulted in a high initial capacity (147 mA h g-1) (Figure 2c-f). Regrettably, there was a small capacity decrease (E42 mA h g-1) following a reversible capacity of B105 mA h g-1 in 50 cycles. The electroactive MOF cathodes were also built using quinone-type ligands as well as a few additional ligands, such as 1,2,4,5-tetraaminobenzene, tetra thiafulvalene tetracarboxylic acid and tricarboxytriphenyl amine [54]

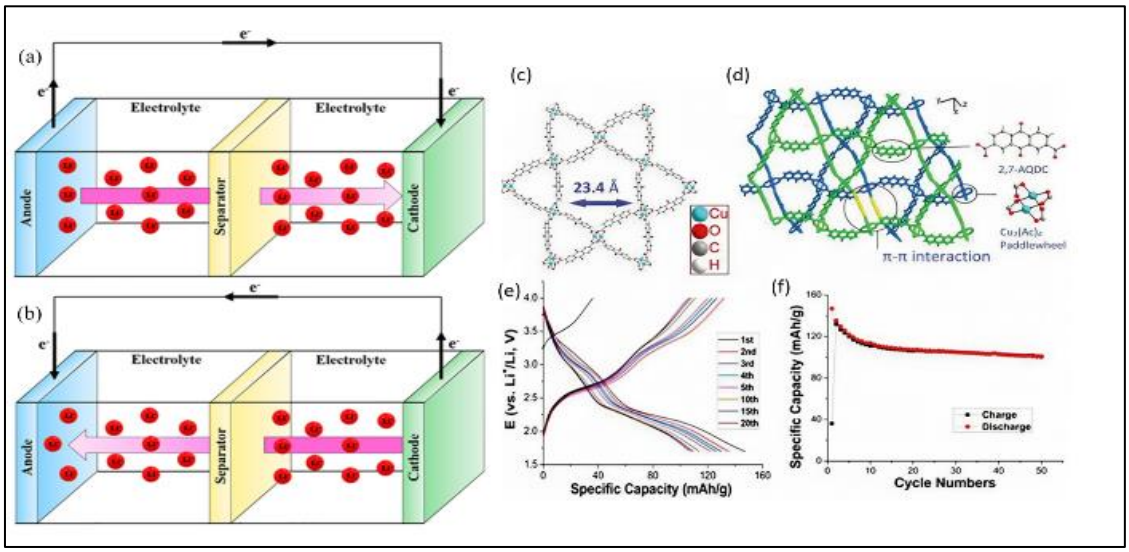

Figure 2 The general mechanism of lithium-ion batteries for discharging and (b) charging processes [55]. (c) The single Kagome layer of Cu(2,7-AQDC) in a battery. (d) The indication picture of the glided adjacent layers. (e) Charge–discharge profiles of the 10 wt% MOF battery. (f) Cycle performances of the battery for 50 cycles [53]

Lin et al. [56] created a highly promising heterotrimetallic Cu-Zn Co MOF grown on copper foam (CF) with interweaving copper nanowires (CNWs) as a LIB anode (CNWs/CZCOZ/CF). Without the need for binders or conductive additives, CNWs/CZCOZ/CF was constructed directly as a functioning electrode. Figure 3(a) shows that using CNWs/CZCOZ/CF as a LIB anode yields an outstanding capacity (2305 mAh g-1) after 500 cycles at a fixed current density of 0.1 A g-1. Interestingly, the electrode maintains a high capacity even at 10 A g-1. Upon reverting back to 0.1 A g-1, the electrode exhibits excellent rate capability as it nearly regains its original capacity as illustrated in Figure 3(b). The outstanding rate performance and cycling stability are credited to the synergic effect between the active multicomponent metal oxide composites [57], which ameliorates the electrical conductivity and rate capacity of the trimetallic MOF derived electrode. Unsurprisingly, when compared to monometallic and bimetallic electrodes (CNWs/ZnO/CF, CNWs/Co3O4/CF, and CNWs/ ZnCo2O4/CF), hetero trimetallic CNWs/CZCOZ/CF electrode displayed a far superior capability. Additionally, the MOF derived electrodes are rich with pores, which not only increases the area of contact between the electrolyte and active material, but also presents void space to relieve volume changes. Finally, the CNWs/CZCOZ/CF also shows an ‘‘electron-sharing” (Figure 3c), whereby Li is less electronegative as compared to Cu, Co, Zn and Li2O, enabling them to obtain more electrons from Li [56].

In another study, a C/N doped trimetallic MOF-derived Cu0.39Zn0.14Co2.47O4-CuO material interwoven with carbon nanotubes on copper foam (CZCOC@CNTs/CF) was used directly as an electrode in LIBs, free from binder and conductive agent. Under the density current of 5 A g-1, the obtained material revealed an excel lent specific capacity of 1282 mAh g-1 over 1000 cycles. One of the main reasons for a high electrochemical performance of CZCOC@CNTs/CF concerns a synergic effect of multimetal oxides that can enhance a high-rate performance and capacity. As observed from the EDS elemental mapping images (Figure 13d), it is obvious that Zn, Co, Cu, C, and N are evenly distributed through-out the electrode. Thus, the synergic effect of Cu, Zn and Co centers that display electrochemical activity toward

lithium is responsible for enhancing the lithium-ion storage capacity [58]. The C/N elements in nanoscale architectures can provide faster and shorter diffusion paths, as well as volume space to compensate for unavoidable volume variance. Metallic Cu, Zn, Co, and LiZn species are produced as a result of irreversible lithiation/delithiation reactions (Figure 3e). In addition, a probable electrochemical mechanism of "electron-shared metal-Li+ capacitor" was postulated, indicating toward extraordinary lithium storage via formation of electric double layer capacitors. On the interface of hybrids, multifunctional Li+ ions form an electric double layer via attachment and adsorption to maintain the charge balance, thus encouraging the sharing of capacitive lithium storage [59].

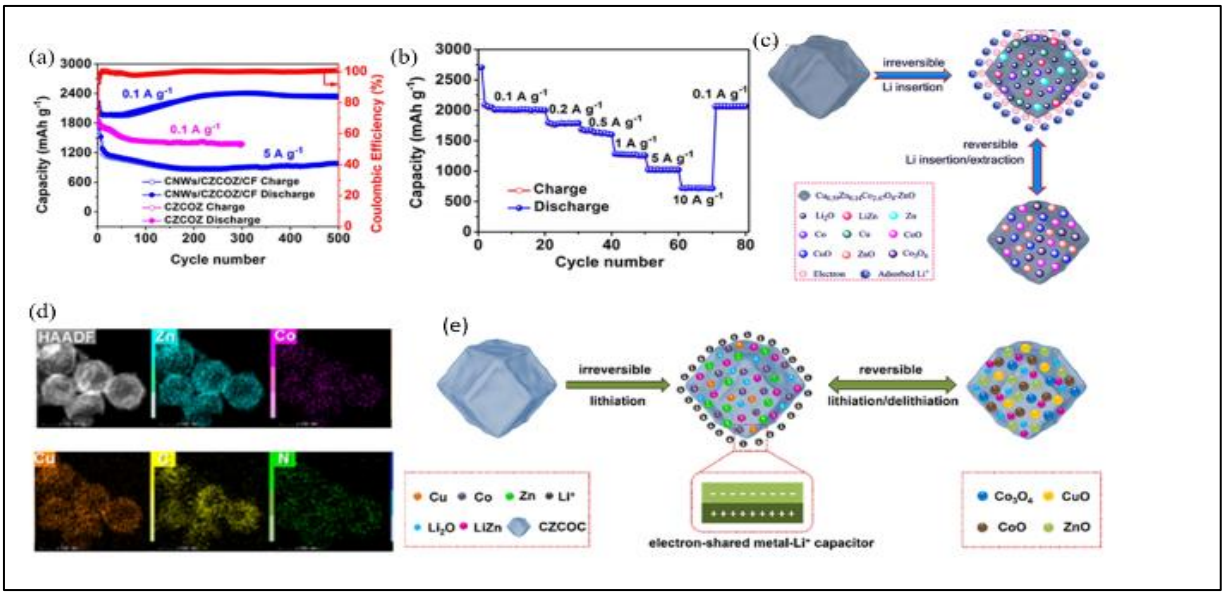

Figure 3 a-c) Key characteristics of CNWs/CZCOZ/CF: (a) Cycling stability and coulombic performance efficiency, (b) rate capability at different current densities, and (c) schematic representation of the "electron sharing" model for charge/discharge operations [56] (d) (d) EDS elemental pictures, (e) synergic effect of CZCOC@CNTs/CF during the lithiation/delithiation process [59]

2.3. MOFs in Sodium-Ion Batteries (SIBs)

SIBs, with their massive reserves, low cost, and little environmental impact, are beginning to show potential as a lithium alternative in energy storage systems. Sodium-ion batteries are particularly appealing since sodium is more readily available and less expensive than lithium, and the extraction method is more sustainable and less harmful [60]. In 2017, Dong et al. [61] successfully synthesized a ZnS Sb2S3@Ccore-double shell polyhedron structure utilizing a zeolitic imidazolate framework (ZIF-8) as the template, as illustrated in Figure 4a. The polyhedron was generated by a sulfurization reaction involving dissociated Zn2+ ions from ZIF-8 and S2− from thioacetamide, followed by a metal cation exchange between Zn2+ and Sb3+. A protective carbon layer was introduced using polymeric resorcinol-formaldehyde, which prevented the polyhedron structure from collapsing. This novel strategy produced a composite with a ZnS inner core and a Sb2S3/C double shell that functions as an anode for sodium-ion batteries (SIBs). Figure 4b depicts the core-double shell structure, demonstrating its excellent homogeneity and dispersion. ZnS Sb2S3@C core-double shell composite is formed by the self-assembly of a ZnS inner core and Sb2S3 inner shell that are connected to the C outer shell. The design demonstrated significantly enhanced electrochemical performance, including high specific capacity, stable cycling, and excellent Coulombic efficiency. The carbon shell not only provided structural stability during Na-ion insertion/extraction but also enhanced electronic conductivity, improving the overall cycle stability and rate capability as per Figure 4c,d. This methodology opens new avenues for developing metal sulfide-based nanostructures for high-performance energy storage devices.

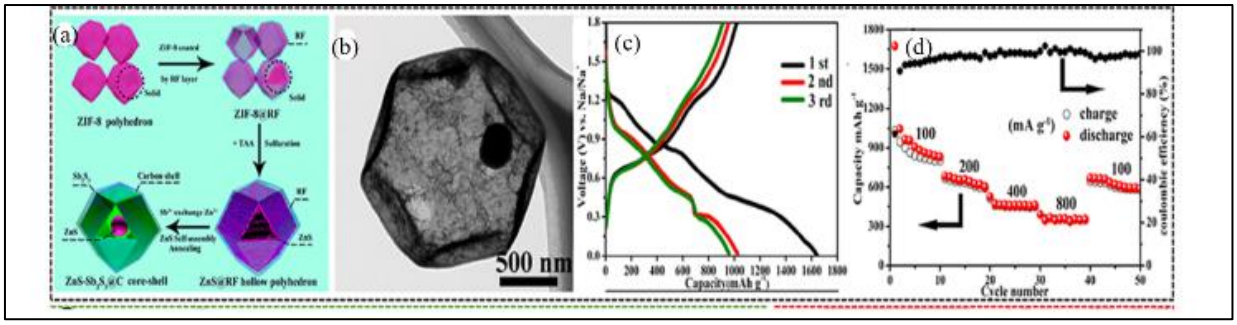

Figure 4 Synthesis of ZnS-Sb2S3@C Core-Double Shell Polyhedron Composites. b) TEM of core double shell c,d) charge/discharge curve and rate capabilities at a current density of 100 mA/g-1 [61]

Yue et al. [62] present the synthesis of a novel porous core shell structure, SnPS3@C as shown in Figure 5a, designed to overcome the challenges faced by metal thiophosphites in sodium-ion batteries, such as sluggish reaction kinetics and severe volume expansion. The SnPS3@Ccomposite is fabricated by phosphor-sulfurizing resorcinol-formaldehyde-coated tin metal organic framework cubes, resulting in a material that features a 3D porous architecture and a robust carbon shell. The porous structure facilitates faster ion diffusion, while the carbon layer enhances electrochemical activity and reduces polarization, addressing the limitations of low conductivity and the inherent conversion-alloying mechanism of metal thiophosphites [63]. Yue et al. also provide a comprehensive investigation of the sodium storage mechanism as shown in Figure 5b through insitu and ex situ characterizations, shedding light on the structural and electrochemical behavior of the material. As a result, the SnPS3@C electrode demonstrates superior electrochemical performance compared to pure SnPS3. The CV profiles of SnPS3@C in a volt age window of 0.01–3 V are depicted in Figure 5c. The galvanostatic charge-discharge (GCD) profiles of the SnPS3@C electrode are illustrated in Figure 5d during the first, second, third, and fifth cycles. Notably, it achieves excellent rate capabilities, delivering 1342.4 mAh g-1 at 0.1 A g-1 and 731.1 mAh g-1 at 4 A g-1 as shown in Figure 5e,h. Furthermore, the electrode exhibits remarkable long-term cycling stability, with 97.9% capacity retention after 1000 cycles at 1 A g-1. This work highlights an innovative strategy for improving the performance of metal thiophosphites by incorporating a porous core–shell structure, which enhances ion transport and stability, making SnPS3@C a promising candidate for advanced sodium-ion battery applications

In a recent study, Wang et al. [64] reported the development of a metal–organic framework (MOF)-derived strategy to synthesize carbon encapsulated yolk-shell nickel-based compounds as anode materials for sodium-ion batteries. Through an in situ con version process, the nickelic MOF precursors are transformed into hierarchical yolk-shell structures of Ni2P/C, NiS2/C, and NiSe2/C by phosphorization, sulfuration, and selenation reactions, respectively Figure 5i. The resulting materials retain their yolk-shell morphology as shown in Figure 5j–l and are encapsulated in carbon, enhancing their electrochemical performance. Among the three synthesized compounds, Ni2P/C demonstrates superior electrochemical properties, including lower polarization, a smaller voltage gap, and faster reaction kinetics compared to NiS2/C and NiSe2 /C. Specifically, Ni2P/C exhibits an impressive initial specific capacity of 3222.1/1979.3 mAh g-1 and a high reversible capacity of 765.4 mAh g-1 after 110 cycles at a current density of 0.1 A g-1. These values significantly outperform the sodium storage capacities of NiS2/C (706.4 mAhg−1) and NiSe2/C (735.8 mAhg-1) Figure 5m–p. This work not only highlights the superior performance of Ni2P/C over its sulfide and selenide counterparts but also demonstrates the advantages of the highly active phosphide phase, large specific surface area, and improved kinetics. The study provides valuable insights into phase and structure engineering for carbon-encapsulated transition-metal compounds, presenting a versatile MOF-derived approach that could be extended to other energy storage materials in advanced battery systems [65].

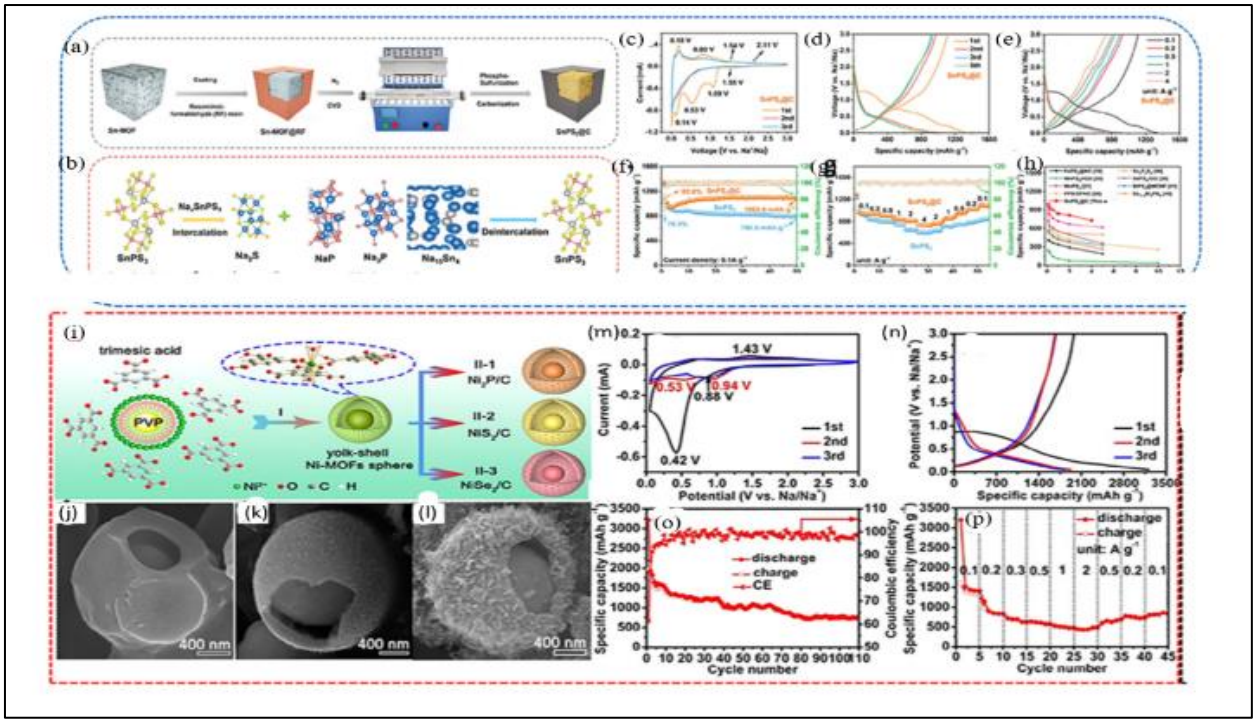

Figure 5 Design of Porus core shell structure of SnPS3@C b) Sodium storage mechanism in the SnPS3@C electrode. Initial CV curves for SnPS3@C electrode. GCD curves for SnPS3@C electrodes at 0.1 A g-1 current density and varied current densities. f) Cycling performance of SnPS3 and SnPS3 @C electrodes at 0.1 A/g. g) SnPS3 and SnPS3@C electrode performance. h) Comparison of SnPS3 @Celectrode rate performance with MTP-based SIB anodes [62] i) Schematic depicting the manufacture of carbon-encapsulated yolk-shell nickelic spheres: (I) hydrothermal method, (II-1) phosphorization, (II-2) sulfuration, and (II-3) selenation reaction. j-l) SEM pictures of Ni2P/C, NiS2/C, and NiSe2/C. m) The first three CV curves at 0.1 mVs-1. n) The corresponding cycle curves. o) Cycle performances at 0.1 Ag-1. p) Rate capabilities with varied current densities of 0.1-2 Ag-1 [64]

2.4. MOFs in Lithium-Sulfur (Li-S) Batteries

Lithium–sulfur batteries (LSBs) are from reserves of active sulfur materials that have shown high specific capacity [66]. They, however, suffer from drawbacks such as the poor conductivity of sulfur and volume change during the charge discharge process. On the other hand, they can result in poly sulfide intermediates, which may dissolve in the electrolyte, leading to the shuttle effect. The mentioned weaknesses have hindered the commercialization of these batteries. In this regard, using cathode materials can decrease the polysulfide diffusion and enhance the conductivity, which will be helpful. Thanks to their high specific surface area, porous structure, and adsorption ability, MOFs can effectively immobilize lithium polysulfide intermediates and, thus, improve the stability of the batteries [67]. In this context, the design of a MOF-based sulfur host in which the features of MOFs are maintained could be highly efficient.

Yang et al. [68] designed V-MOF (MIL-47)-derived V2O3@C hollow microcuboid (Figure 6a) and used it as a sulfur host. The hollow micro cuboid morphology with a hierarchical lasagna-like structure provides channels for ion transport. At the same time, carbon framework physical confinement and V2O3 chemical adsorption prevented the shuttle effect, giving rise to good cycling stability for the V2O3@C/S composite cathode (Figure 6b). In another study by Chen and colleagues, density functional theory was employed to assess two-dimensional porphyrin-like MOFs. Their results indicated remarkable chemical interactions of V-MOFs with lithium polysulfides, which decreased the shuttle effect, improving the performance and increasing the energy density [69]. In 2021, the synthesis of MnM-MIL-100 bimetallic was carried out by Li et al. with no changes in the main morphology to store the electrochemical energy (Figure 6c and d). The MnNi-MIL-100@S cathode had the most optimum performance of Li–S batteries, indicating an approximately 708.8 mA h g-1 reversible capacity following 200 cycles [70].

Furthermore, Hong et al. [71] found that 100 nm-sized nano particles outperformed 200 nm-, 500 nm-, and 1 mm-sized particles for a Cu-MOF that used both ligand Lewis acid sites and node Cu sites for polysulfide interaction. Electrochemical reactions only take place on the particle surface, where electrons and Li ions are accessible due to the

conductivity constraints of the MOFs in both scenarios. The electrochemical performances of recent MOFs materials for Li–S batteries are summarized in Table 2.

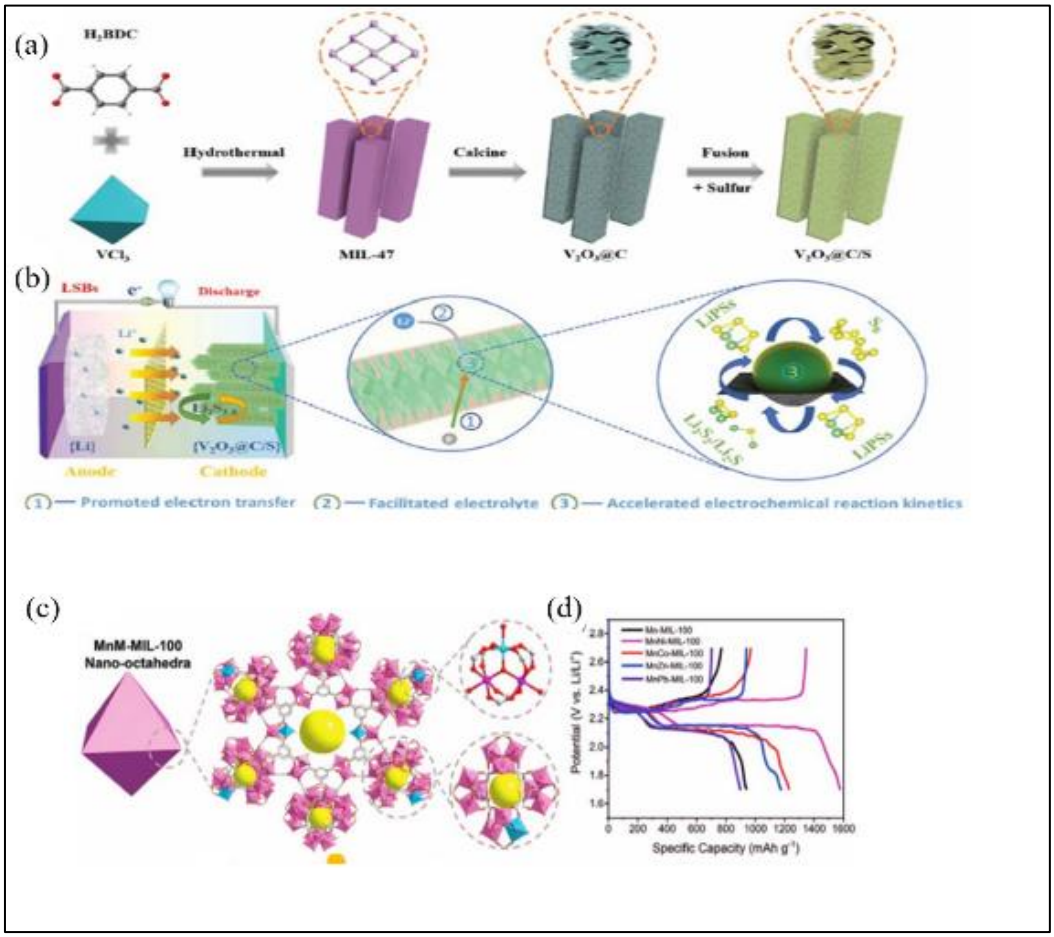

Figure 6 Three main properties of the V2O3@C/S electrode material; (b) fabrication process of the V2O3@C/S [68]. (c) Preparation of MnM-MIL-100 and (d) GCD profiles at a current density of 0.1C. [70]

Table 2 Performance Metrics of Selected MOF-Based Materials in Lithium-Sulfur Batteries

MOF Used	S loading	Current density	Cycle number	Voltage vs. Li/Li^+ [V]	Specific capacity [mA h g^{-1}]	Ref.
ZIF-8	54wt%	0.2C	1000	1.4-3.0	=170	[72]
MIL-100(Cr)	48wt%	0.1C	60	1-3	=410	[73]
ZIF-8	30wt%	0.1C	100	1-3	=510	[74]
ZIF-8	50wt%	0.5C	300	1.8-2.8	553	[75]
HKUST-1	50wt%	0.5C	300	1.8-2.8	286	[75]
NH_2-MIL-53	50wt%	0.5C	300	1.8-2.8	332	[75]
MIL-53	50wt%	0.5C	300	1.8-2.8	347	[75]
MIL-101(Cr)	50wt%	0.2C	50	1.5-3.0	650	[76]
$Ni_6(BTB)_4(BP)_3$	60wt%	0.1C	100	1.5-3.0	611	[77]
MIL-101(Cr)	58.8wt%	0.8C	134	1-3	809	[67]
MOF-525	50wt%	0.5C	200	1.5-3.0	700	[78]

3. MOFS in Zinc Batteries (ZBs)

Zinc (Zn), abundant in the Earth's crust, is widely recognized for its diverse applications in energy storage. With a redox potential of 0.763 V relative to the standard hydrogen electrode (SHE), zinc offers high theoretical capacities of 5854 mAh/cm3 and 819 mAh/g. Zinc's stable and eco-friendly supply chain further enhances its attractiveness for energy storage technologies. Recent advancements in the protection of Zn anodes and electrolytes have revitalized interest in zinc-based energy storage systems [79]. Among the various aqueous zinc-based electrochemical energy storage (EES) devices, zinc-air batteries (ZAB) and aqueous Zn-ion batteries (AZIB) show significant promise in meeting the demands for higher energy and power densities, respectively [80]. Before zinc-based systems can commercially challenge lithium-ion batteries (LIB), significant advancements in cathode materials are essential. It has been established that Zn anodes are compatible with aqueous-based electrolytes, making them suitable for various battery types, including Zn-air, nickel-zinc, and zinc-manganese batteries [81]. The sustainability, eco-friendliness, and performance of Zn-based batteries are drawing considerable interest in these recent years. Alkaline zinc/manganese dioxide cells, a fundamental form of early batteries, have garnered scientific attention due to their numerous advantages, such as cost-effectiveness, ease of assembly, safety, a two- electron transfer mechanism, and the abundant presence of elemental Zn in the Earth's crust. These benefits have recently spurred significant interest in rechargeable ZIBs with moderate aqueous electrolytes (pH ≈ 7). Metallic Zn is considered an excellent anode material for aqueous ZIBs [82].

The choice of electrolyte is crucial in determining the functionality of AZIBs. Aqueous electrolytes provide similar advantages, such as excellent ionic conductivity, affordability, and environmental friendliness. Anolyte compositions commonly consist of aqueous solutions containing Zn salts, such as Zn sulfate or Zn chloride [83]. These solutions facilitate the movement of Zn ions between the electrodes. Figure 7b shows the mechanism of ZIB. Furthermore, compared to LIBs, which have an energy density range from 100 to 265 Wh kg-1, ZABs have the capacity to generate a substantially greater energy density of 1353 Wh kg. Commercial primary ZABs have continuously produced high energy densities between 200 and 500 Wh kg-1 since their inception. Rechargeable ZABs haven't shown much commercial availability, though [84]. Even the newest commercial devices have a rather low cycling durability and energy density. Two main causes of their poor electrochemical performance are (1) thermodynamic instability in electrolytic solution of anode made by Zn; and (2) the controlled quantity of active sites regions present on bifunctional air cathodes [85]. The structure of ZAB is shown in Figure 7a.

However, despite the progress made, issues related to the stability and performance of Zn anodes persist. MOFs and their derivatives have shown considerable promise in addressing these challenges. The numerous active sites, large surface areas, and flexible, uniform porous structures of MOFs contribute to the superior performance of electrolytes, porous carbon materials, and electrolytic compounds [86]. From a materials science and chemistry perspective, the active sites in MOFs, often composed of transition metals like Co, Fe, Ni, and Mn, serve as catalysts for the oxygen reduction reaction (ORR) and the oxygen evolution reaction (OER). These metals facilitate the adsorption and reduction of oxygen molecules during discharge and their evolution during charging. Organic ligands enhance catalytic activity by providing additional coordination sites and stabilizing intermediates [87].

Recent studies have highlighted specific examples of MOFs and their applications in electrochemical systems: Zhang et al. demonstrated the effectiveness of cobalt-based MOFs as bifunctional catalysts for ORR and OER, showing improved stability and performance in ZABs [88]. Figure 7 presents a comprehensive study on V-MOF-48 and its application in energy storage, particularly in zinc-ion batteries. Figure 7c illustrates the growth stages of V-MOF-48 over time, showing a seed-like structure that evolves into a more complex, hierarchical form over 48 h. By 12 h, the initial growth is visible, and by 24 h, the structure is more developed, finally reaching its fully grown form at 48 h. Figure 7b provides a Scanning Electron Microscope (SEM) image of the V-MOF-48 after 48 h of growth, revealing a porous, tree-like morphology beneficial for high surface area applications in energy storage. Figure 7c compares the electrochemical performance of different V-MOF-48 materials with varying Zn content (labeled as V-MOF-48/Zn). The graph plots potential (V) versus capacity (mAh/cm3) for each sample, illustrating the energy storage capabilities and efficiency under electrochemical cycling. Figure 7d schematically depicts the composite electrode structure, comprising V- MOF-48, Zn nanosheets, a PVA (polyvinyl alcohol) electrolyte, and CNTFs (carbon nanotube fibers). This illustration highlights the integration of these materials into a cohesive electrode design, emphasizing their interaction to enhance performance. Figure 7e displays charge- discharge curves at different current densities, ranging from 0.1 A/ cm2 to 5.0 A/cm2. Each curve represents the potential (V) versus capacity (mAh/cm2) during the charge and discharge cycles, demonstrating the battery's performance variations with different current densities and indicating the rate capability and stability of the V-MOF- 48 based electrode. Finally, Figure 7f presents performance metrics over various current densities, with a graph showing capacity (mAh/cm2 and capacity retention (%) as functions of the current density (A/cm2)). The blue line with triangles indicates capacity, while the red line with circles shows capacity retention, demonstrating how capacity decreases with

increasing current density and providing insights into the electrode material's durability and efficiency under different loading conditions [89].

These studies underscore the versatility of MOFs in addressing critical challenges facing ZABs, including electrode stability, catalytic efficiency, and overall battery performance. Future research efforts may focus on further optimizing MOF properties, exploring new composite materials, and scaling up production methods to accelerate the integration of MOFs into commercial zinc-air battery technologies. Table 3 shows the performance metrics of selected MOF-based materials in zinc-ion batteries

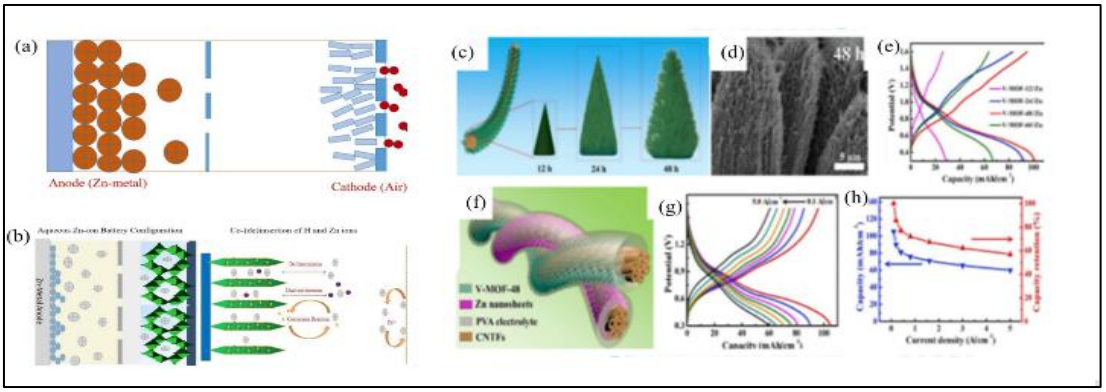

Figure 7 Zn-air battery schematic representation (b) Mechanism of aqueous Zinc-ion battery [90]. (c) A diagram of the process for producing the Vanadium-MOF@CNTF, which has a nanowire structure. (d) SEM picture of vanadium-MOF 48. (e) V-MOF-60//Zn, V-MOF-48//Zn, V-MOF-24//Zn, and V-MOF-12//Zn galvanostatic charge-discharge curves measured at 0.1A/cm. (f) Illustration of the all-solid-state fiber-shaped V-MOF-48/Zn battery. (g) The galvanostatic charge-discharge curves, and (h) fiber-shaped V-MOF-48//Zn battery specific capacities determined at various current densities [89]

Table 3 Performance Metrics of Selected MOF-Based Materials in Zinc-Ion Batteries

Electrode	Capacity (mAh/g)	Cycling stability	Current density (A/g)	Voltage window (V)	Ref
Mn-H_3BTC-MOF-4	138	93.5 % after 1000 cycles at 3 A/g	0.1	1.0–1.9	[91]
Mn_3O_4@C	331.5	141 % after 1900 cycles at 3 A/g	0.2	0.8-1.8	[92]
CoMn-PBA HSs	128.6	75.4 % after 1000 cycles at 1 A/g	0.05	0.4–1.8	[93]
MnOx@N-C	203	105 % after 1600 cycles at 2 A/g	0.1	0.8–1.8	[94]
$Cu_3(HHTP)_2$	228	75 % after 500 cycles at 4 A/g	0.05	0.5-1.3	[95]
VHCF	176	92.9 % after 1000 cycles at 5 A/g	0.2	0.2–2.0	[96]
Mn_2O_3/Al_2O_3	90	57.1 % after 1100 cycles at 1.5 A/g	0.3	1.0–1.8	[97]
Mn-Co-O@C	306	94.7 % after 2000 cycles at 2 A/g	0.5	0.8–1.9	[98]
$CoFe(CN)_6$	173.4	100 % after 2200 cycles at 3 A/g	0.3	0.7–2.0	[99]
KMHCF	123.8	90 % after 500 cycles at 0.25 A/g	0.05	1.0–2.0	[100]

3.1. MOFs for Supercapacitor Applications

Ultracapacitors (electrochemical capacitors), also recognized as supercapacitors, are high-power capacitors with a long-life cycle, which have attracted significant research attention in the past few years [101]. In recent years, they have been identified as effective replacements for batteries due to their excellent electrochemical characteristics [102]. Firstly, SCs offer very fast charging and discharging rates, providing a massive power density (PD) above 10 kW kg-1, which is approximately 10–100 times greater than that of batteries [103]. Secondly, SCs can effectively function in a broad operating temperature span from 40 ◦ C to 70 ◦ C [104, 105]. Thirdly, they undergo negligibly phase changes during charging and discharging, allowing them to withstand up to 1,000,000 cycles, significantly more than batteries, which typically endure about 1000–10,000 cycles [106]. SCs act as a bridge, addressing the power-energy disparity between capacitors, which have high PD, and fuel cells/batteries, which have larger energy storage capacities [107]. SCs are primarily categorized into two distinct classes depending on their CSM: 1) EDLCs, which exhibit non-faradaic behavior, and 2) PCs, characterized by faradaic behavior. The combination of EDLCs and PCs behaviors has contributed to the breakthrough of a new type of SCs called hybrid supercapacitors (HSCs), which significantly overcome the drawbacks associated with both EDLCs and PCs (Figure 8a). SCs contain electrodes that are typically composed by active carbons (AC) with a large surface area, a separator to avoid short circuit, and an electrolyte (aqueous or organic electrolytes or ionic liquids) (Figure 8b). These devices store electrical energy at the interface between the electrode and the electrolytic solution, in a region termed as the electrical double-layer (EDL) [108].

In the EDLC mechanism, a double layer of charge forms on the boundary surface of electrode and electrolyte, based on a non-faradaic redox reaction, whereas in the pseudocapacitive mechanism, the active material undergoes a faradaic redox reaction [109]. Previous literatures have revealed that electrode material is one of the most important factors affecting the electrochemical performance of SCs. EDLCs generally employ carbon-based materials with high surface area and adequate porosity, such as carbon nanotube (CNT), graphene, and activated car bon (AC), while transition metal oxide (MO), transition metal hydroxide, and conductive polymer are usually served as electrode materials in faraday pseudocapacitors [110]. Varying from EDLCs and pseudocapacitors, HSCs are composed of capacitor-type electrodes and battery- type electrodes, utilizing two different reaction mechanisms (non-faradaic redox reactions and faradaic redox reactions) to achieve high specific energy and specific power simultaneously. Moreover, SCs can also be classified into symmetric and asymmetric supercapacitors according to the different active materials. The symmetric supercapacitors have the same positive and negative active materials, while asymmetric supercapacitors (ASC) have different positive and negative active materials. Compared with symmetric supercapacitors, the ASCs assembled with battery-type electrode and capacitive electrode not only broaden the operation voltage, but also greatly improve specific capacitance and energy density [111].

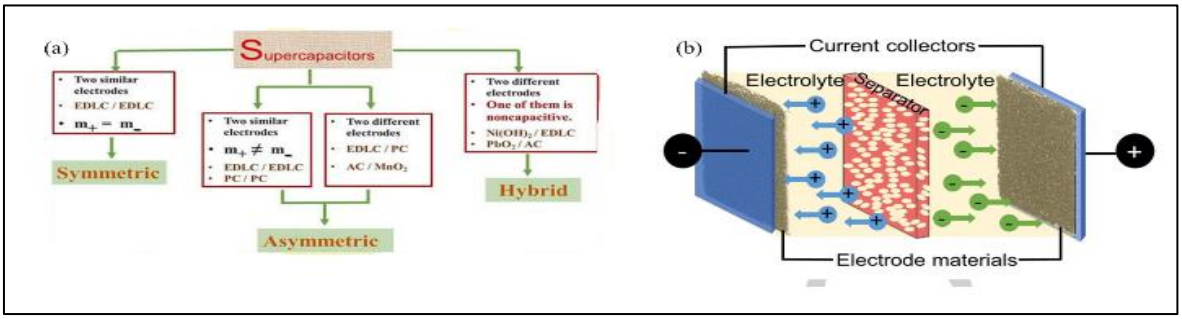

Figure 8 Configuration of the electrode assembly of SCs [112] (b) Schematic illustration of a SC and its individual components [108]

The high performance of SCs is heavily influenced by the choice of battery-type electrode material. However, conventional battery-type electrode materials such as TMOs, TMCs, TM nitrides, TM phosphides, and CPs often do not meet the requirements due to a lack of electronic conductivity, low CS, and less cycling stability [113]. Hence, there is a demand to construct high-performance electrodes for SCs. In this context, MOFs have garnered significant attention in the research community. MOFs are composed of metal centers connected by organic molecules through strong covalent bonds. TMs, alkaline earth metals, or lanthanides typically serve as the metal centers, while organic linkers usually contain 'O' or 'N' donor atoms. By selecting specific metal ions and organic linkers, MOFs can form 1D, 2D, and 3D networks with customizable structures, making them suitable for SCs [114]. Their dimensionality and porosity improve ion transport and energy storage. The bandgap of MOF-based semiconductors, ranging from 1.0 to 5.5 eV, can be adjusted by modifying ligands and reaction conditions. π-conjugated MOFs enhance charge-carrier mobility and conductivity, crucial for SCs performance [115].

Many research reports have shown that MOFs-derived metal-(oxides, sulfides, nitrides, phosphides and oxide/ carbon) composites serve as suitable electrodes for SCs applications. MOFs offer numerous advantages, including their ability to serve as electrodes themselves, act as precursors for synthesizing metal oxides and sulfides, and transform into metal oxide composites, including metal oxide/carbon composites, after pyrolysis at high temperatures. Direct MOFs electrodes provide ample space for electrolyte ion adsorption and lead to effective redox reactions due to their porous network structure [116]. Moreover, MOFs-based electrode materials deliver good electrochemical performance due to their interlayer structures and redox-active sites, resulting in high Cs, high reversible capacity, and high-rate capability with good cycling performance [117, 118]. However, coordination polymers have limited application in energy storage owing to their weak conductivity and inferior thermal stability [119].

Yuan et al. employed a hydrothermal method to prepare NiCo-LDH@C nanostructures using a carbonized flake ZIF-67 template. The uniformly distributed Co@C provided nucleation sites for NiCo-LDH formation, resulting in a hierarchical structure anchored to the carbon skeleton (Figure 9a) [120]. In another method, Panda et al. successfully synthesized ultrathin bimetallic NiCo-MOFs-31 through a solvothermal method (Figure 9b) [121]. To enhance the stability and conductivity of MOFs, they were integrated with conductive polymer porous carbon nanofibers (PCNFs) decorated with Fe-MOFs NRs through a hydrothermal method [122]. Increasing metal salt concentrations accelerate proton (H+) expulsion from hydrolysis, leading to the etching of Fe- MOFs@PCNFs and the co-precipitation of Fe and Ni ions, forming layered hydroxide. However, excessive concentrations expel too many H+ , causing excessive Fe3+ removal and self-aggregation of Ni(OH)2, which results in unfavorable layered structures in Ni-Fe-OH@PCNFs. The NiFe OH@PCNFs electrode material possessed a porous architecture with a high SSA, promoting high ion/electron transportation, contributing to achieving an excellent Cs of 1528 F g-1 at 1 A g-1 with outstanding cycling stability of 86.7 % over 10,000 cycles. After 10,000 cycles, Ni-FeOH@PCNFs-1 exhibited lower Rs (3.09 Ω) and Rct (2.73 Ω) than MOFs or partial layer hydroxide. The Ni-FeOH@PCNFs-1 electrode maintained steady conductivity and minimal resistance increase compared to other electrodes (figure 9c) [122].

Interestingly, Sun et al. proposed a facile two-step approach (Figure 9d), deriving copper cobalt selenide ((CuCo)Se) from CuCo-ZIF-0.5. This approach delivered a reasonable Cs of 121.4C g-1 at a current density of 1 A g-1 and a capacitance retention of 82 % [123]. Here, (CuCo)Se NPs were embedded in NC through MOFs. It is important to note that the optimized Cu species insertion into CoSe matrices with the coupled NC layers ((CuCo)Se/NC-0.5) displayed low Rct, inferring high Cs, stability, and rate capability for a high-performance practical device. Moreover, Xu et al. precisely assembled a 3D flower-like structure resulting from NiFe2O4 quantum dots (QDs) anchored on Ni-MOFs NSs prepared by the solvothermal method (Figure 9e). The Ni-MOFs NSs provided effective accommodation for uniformly anchored QDs, excellent dispersion, and protection from aggregation [124].

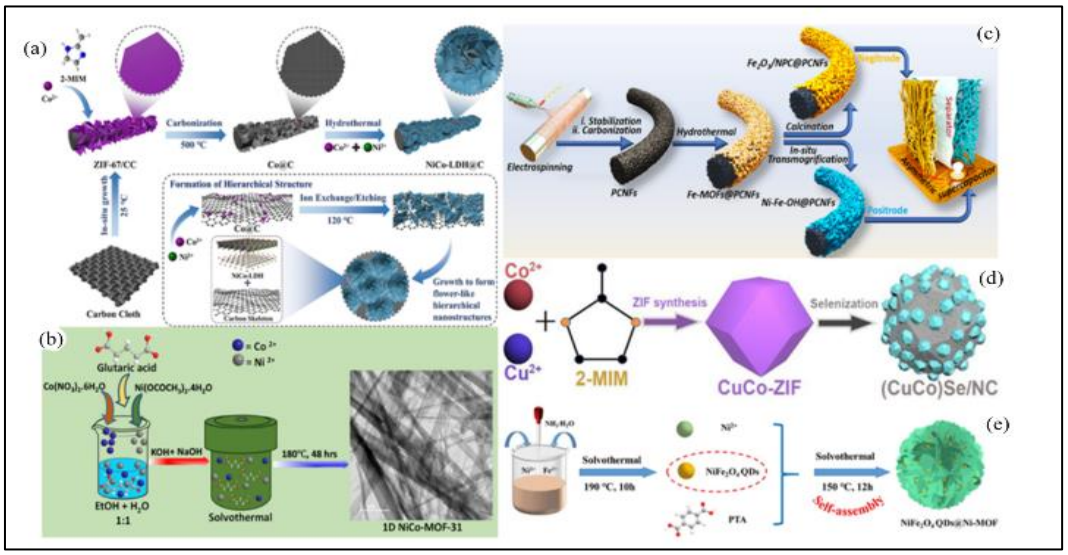

Figure 9 Schematic sketch of the process MOFs derived NiCo-LDH@C [120] b) Illustration of the preparation of NiCo-MOFs-31 [121] c) Schematic drawing of the fabrication of the Ni-Fe-OH@PCNFs electrode for the ASC device [122] d) Graphical representation of the preparation of (CuCo)Se/NC nanocomposite [123] e) Graphical design of the construction of NiFe2O4 QDs@Ni-MOFs [124]

The combination of various MOFs with highly conductive systems such as conductive polymers and graphene has been proved to be a novel approach to increase the performance of SCs by boosting the conductivity of MOFs. Choi et al. appropriately doped graphene into 23 crystalline metal–organic systems to create SCs [125]. Many nanocrystalline MOFs with diverse pore sizes have been studied thus far. One of the most successful nanocrystals, i.e., [Zr6O4(OH)4(BPYDC)6]n (where BPYDC is 2,2′-bipyridine-5,5′-dicarboxylate) exhibited the highest SC capability over 10000 cycles with a given stack and areal capacitance of 0.64 and 5.09 mF cm-2, respectively, thereby showing great material strength. Owing to their high porosity, MOFs also possess enormous electro-chemical double-layer capacitor-type capacitance under similar conditions due to which electrolyte ions can easily diffuse through their micro- and mesopores [126].

ZIF67 nanocrystals electrochemically interacted with conductive polyaniline (PANI) to improve their conductivity. Consequently, a high areal capacitance of about 2145.9 mF cm-2 at 9.9 mV s-1 was shown by PANI-77 by supporting electron transportation by directly linking the metal–organic system with external simulation. Thus, organic polymers and metal oxides can also be used for integrating MOFs and pseudocapacitor materials [49]. In a recent report studying the behavior of an electric double layer capacitor, an advanced conductive MOF, i.e., "[Ni3(HITP)2]n(HITP = 2,3,6,7,10,11-hexaiminotriphenylene)", was also highlighted, as shown in Figure 10. When there are no conductive materials or organic linkers available, an MOF based supercapacitor was developed as a single-material electrode system, resulting in a gravimetric capacitance of roughly 110.9 F g-1 at 0.049 A g-1. These results are comparatively more advanced than that of carbon-based nanotubes. These MOF-based SCs generally show a greater surface area. It has a controlled specific capacitance of about 17.9 mF cm-2, which is generally higher than that of carbon-based nanotubes excluding graphene. An experimental study also suggested that after 10 000 cycles, the capacity retention factor is very high. Properties such as rapid charge and discharge rates, low molecular weight and bipolar operating flexibility are characteristics of carbon-based SCs, which promote the use of MOF-derived nanoporous carbons in capacitive applications [127]. Table 4 provides a summary of further studies assessing performance metrics of Selected MOF-Based Supercapacitors

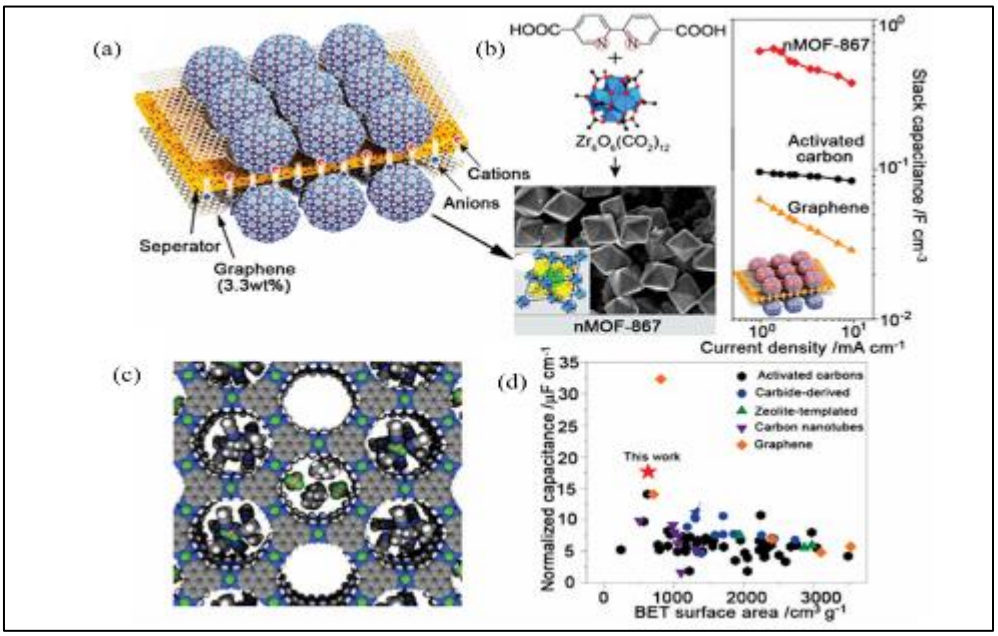

Figure 10 Overview of MOF-based SCs. (a) Representation of nMOF SCs. [125] (b) Structure and nanocrystal topology of nMOF867 with stack capacitances among different EDLC materials. (c) Space-filling view of perfect Ni3(HITP)2 (Ni represents green; F, lime; N, blue; C, grey; B, brown; and H, white). (d) Comparison of the areal capacitances of several EDLC compounds using BET surface area [127]

Table 4 Performance Metrics of Selected MOF-Based Supercapacitors

Electrode	Morphology	Electrolyte	Potential window (V)	Cs	Cyclic stability	Method of Synthesis	Ref.
Ni-MOFs	Hollow nanosphere	3 M KOH	0–0.45	473 @ 0.5 A/g	94 % 3000	Solvothermal	[128]
(CuCo)Se/NC	Polyhedral	2 M KOH	0–0.4	121.4C/g @ 1 A/g	130 % 1200	Salinization	[123]
ZnMn2O4/C	Nanorods	1 M Na2SO4	0–1.2	589 @ 1 A/g	98 % 2000	Facile	[129]
Co-MOFs	Nanorod	3 M KOH	0–0.4	958 @ 2 A/g	92 % 3000	Hydrothermal	[116]
Ni/Co-MOFs-rGO	Particles distributed on Nanosheets	6 M KOH	0–0.6	860 @ 1 A/g	91.6 % 6000	One pot Co-Synthesis	[130]
NiMOFs@NCS/NF	3D porous network	2 M KOH	0–0.6	8.7C cm2 @ 1 mA cm2	89.7 % 5000	Hydrothermal	[131]
Ni-MOFs	Microsphere	6 M KOH	0–0.6	1498 @ 1 A/g	Nil	Hydrothermal	[132]
rGO-NiCo2S4 MOFs	Nanoflakes and sheets	6 M KOH	-0.1–0.45	972 @ 1 A/g	70.5 %	Hydrothermal	[133]
Ni/Co-MOFs/rGO	Spherical and rod	1 M KOH	0–0.5	958 @ 1 A/g	109 % 5000	Chemical	[134]
Ni-Co-S/ACC-MOFs	Nanosheet and Hollow	6 M KOH	0–0.5	2392 @ 1 A/g	85 % 10,000	Hydrothermal	[135]
NiO-MOFs	Cauliflower	2 M KOH	0–0.5	1863 @ 0.5 A/g	82 % 5000	Explosion-Thermolysis	[136]
Co2-Ni-MOFs	Flower	6 M KOH	0–0.6	1300 @ 1 A/g	71 % 3000	Hydrothermal	[137]
CoNi-MOFs	Vertically oriented sheets	1 M KOH	-0.2–0.5	1044 @ 2 A/g	94 % 5000	Electrodeposition	[138]
Ni-MOF@ PEDOT	Nanosheet	0.5 M Na2SO4	-	1401 F/g at 0.5 A/g	80.6 % 1000	In-situ deposition	[139]
CeO2@ ZIF-8		-	-	132 F/g at 1 A/g	90 % 5000	Wet chemical strategy	[140]

3.2. MOFs For Hydrogen Storage

Hydrogen energy is considered to be clean energy because its gravimetric heat of combustion is as high as 123MJmol-1, 3 times higher than gasoline [141]. It is expected to achieve zero emissions during use, making it a new energy source with great development potential. Nonetheless, the current environmental conditions impose constraints on the working volume storage capacity of H2 storage materials, which hinders the widespread adoption of hydrogen energy. The idea of using H2 as a fuel for mobile or portable fuel devices has sparked significant curiosity in H2 storage options. MOF-based hydrogen storage is totally reversible, does not require expensive thermal treatments, and may be recharged in seconds or minutes. This is definitely a benefit over other storage materials, such as metal hydrides. In MOF-5, inelastic neutron scattering was used to reveal the unique positions of adsorbed hydrogen molecules, whereas density functional theory (DFT) calculations suggested that that each Zn4O-cluster could store 16–20 molecules of H2 [101].

The US Department of Energy (DOE) has established weight percentage and density targets for hydrogen storage: 4.5wt%; 30gL1 (2020), 5.5 wt %; 40 g L1 (2025), 6.5 wt %; and 50 g L1 (ultimate). To meet the requirements set by the DOE for on-board hydrogen storage systems, storage materials should possess a high capacity at 100 bar and a low capacity at 5bar. MOF-based materials are anticipated to satisfy these targets and overcome this limitation [142].

In 2003, the Yaghi group first reported Zn4O(bdc)3(bdc,1,4-benzenedicarboxylate) for H2 storage, and revised its hydrogen storage capacity in 2007 [143, 144]. In 2010, they reported MOF-210 with 17.6% of total gravimetric capacity at 77K and 80 bar working conditions [145]. Subsequently, numerous studies have been conducted on MOFs for H2 storage. Nowadays, through advanced methods such as machine learning and high-throughput screening, it is possible to quickly make a preliminary judgment of the gas storage capacity of some new types of MOFs. Scientists have therefore begun to work on clarifying the influencing factors of the gas storage of MOFs and improving the H2 storage capacity of the MOF-based materials in real working scenarios for practical applications. In 2020, the connection between MOFs' void geometry and their overall H2 adsorption was analyzed by Zhang et al. They used a computer to screen six optimal MOFs (HKUST-1, NU-125, NU-1000, UiO-68-Ant, Cu-MOF-74, and Zn2(bdc)2(dabco)(dabco, diazabicyclooctane) for the empirical equations as shown in Figures 11a-g. They concluded that the caged MOFs with a ratio of pore diameter (D) to pore size (A) greater than1.8 adsorb guest molecules more readily than channeled MOFs (D/A = 1). With the help of this empirical equation, they found a caged zirconium-based MOF, NPF-200 (NPF, Nebraska porous framework; Figure 11h), with a specific surface area of 2,268 m2cm3 and a record-level volumetric working capacity (77K, 37.2gL1 adsorption capacity from 5to100bar), particularly greater than that of MOFs with a specific surface area exceeding 3,000m2cm3 [146]. They also reported a kind of microporous aluminum -based MOFs with simultaneous CH4, H2, and CO2 storage capacity and high stability 1 year later. This discovery further confirmed the broad applicability of MOF materials in gas storage research [147].

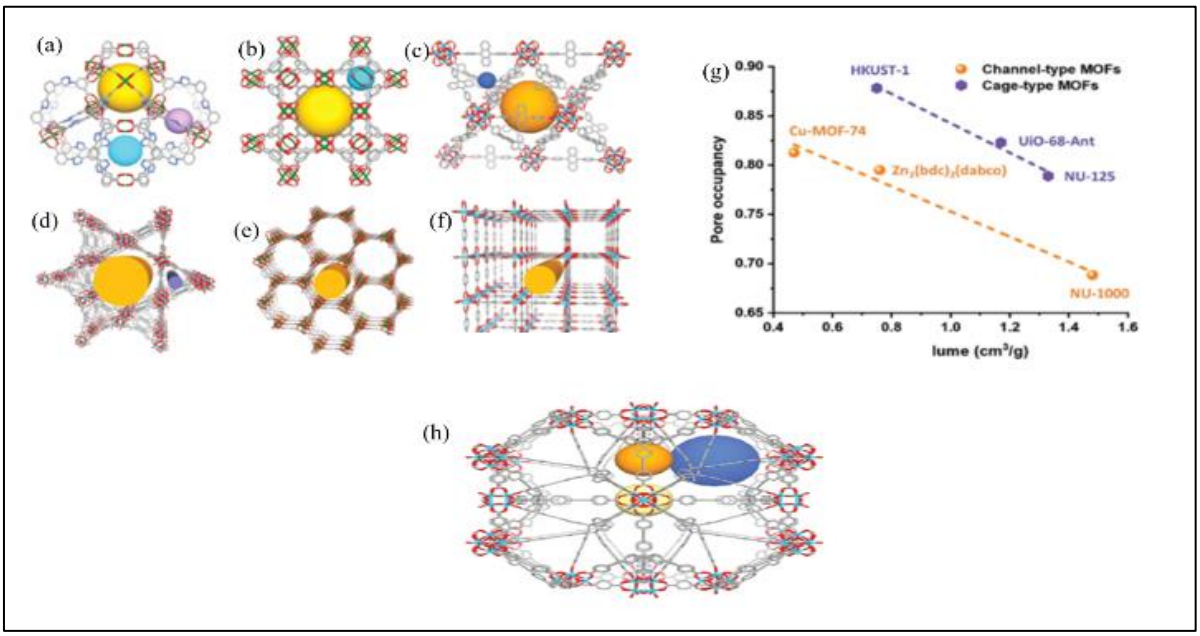

Figure 11 Structural diagrams of six representative MOFs. (a) NU-125, (b) HKUST-1, (c) UiO-68-Ant, (d) NU-1000, (e) Cu-MOF-74, and (f) Zn2(bdc)2(dabco). (G) The plot of pore occupancy versus pore volume for channel-type and cage-type MOFs at 77 K and 100 bar. (h) Three major cages of NPF-200 [146]

Han et al. [148] showed that H2 adsorption mechanisms of MOFs can be modified by changing the aromatic organic linkers by carrying out GCMC simulation which gave a good reproduction of experimentally determined hydrogen loading. Inelastic neutron scattering experiments for Zn-MOF-C6 as a function of H2 loading show that the favored binding site is near the metal clusters, while increased loading leads to additional molecules occupying sites closer to the organic linkers. This finding is consistent with the GCMC simulations, which at 77 K and 0.05 bar show H2 adsorbed only near the metal oxide unit (Figure 12a), while at higher loading (Figure 12b) H2 starts occupying sites on organic linkers. This result is also supported by our MP2 calculations, which indicate that the H2 binding energy is higher with the Zn oxide cluster than with the benzene ring. Thus, for Zn-MOF-C6, although the metal oxide cluster is preferentially responsible for the adsorption at very low pressure (H2 loading), the importance of the organic linker is enhanced with increased H2 loading. For example, at a pressure of 30 bar, the organic linker accounts for 74% of the loading. On the other hand, Zn-MOF-C30 shows a different H2 adsorption mechanism. At 77 K and 0.05 bar, H2 is adsorbed only on the

organic linkers (Figure 12c), while at 0.5 bar it occupies sites both on the organic linkers and near the Zn oxide nodes (Figure 12d, where H2 adsorbed at the metal oxide nodes are shown as green atoms in the expanded view).

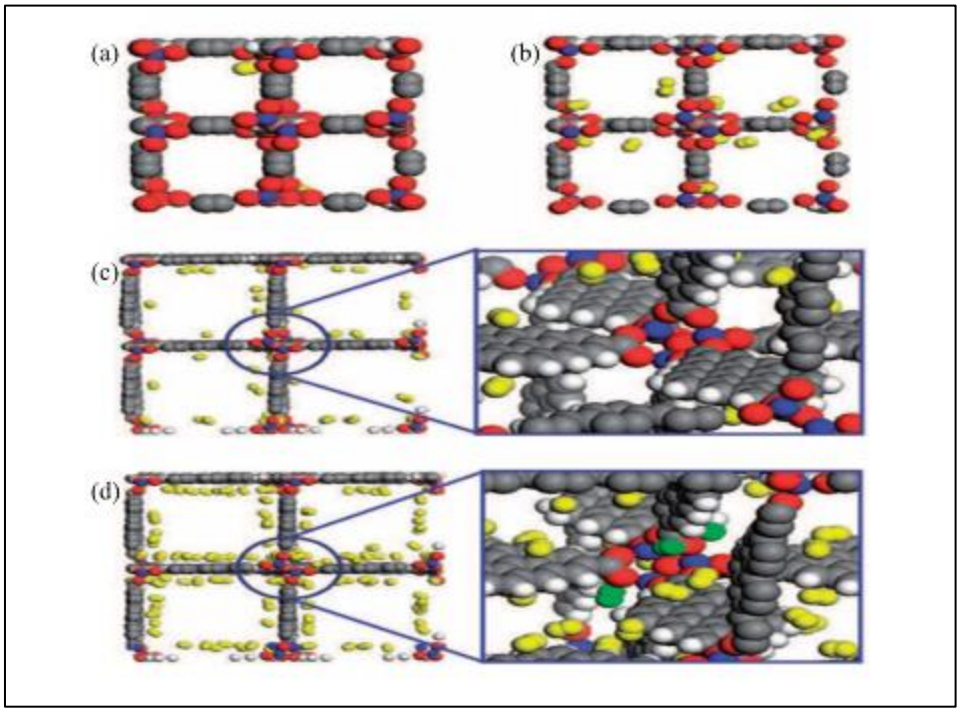

Figure 12 Images of the structures of different MOFs with adsorbed H2 at different pressures. a) Zn-MOF-C6 at P=0.05 bar; b) Zn-MOF C6 at P=0.5 bar; c) Zn-MOF-C30 at P=0.05 bar; d) Zn-MOF-C30 at P=0.5 bar. Zn blue, O red, C gray, H white and yellow. In the expanded view of (d), H2 adsorbed near the ZnO vertices is shown in green. [148]

4. The Computational Revolution in Metal-Organic Framework Design

The new field of Metal-Organic Frameworks (MOFs) consists of an immense chemical space defined by the combinatorial potential of their organic linkers and metal nodes. This enormity, replete with potential for myriad applications, has long presented a formidable challenge to materials discovery, as conventional experimental synthesis and characterization can be time- and resource-intensive. To combat this, computational and Artificial Intelligence (AI)-driven approaches have emerged as key tools, shifting the paradigm from trial-and-error empiricism to accelerated, rationalized design. These state-of-the-art approaches enable high-throughput screening, predictive modeling, and detailed mechanistic investigations, thereby revolutionizing the tempo and precision of MOF research and development [149].

One of the most potent computational advances in MOF design is high-throughput screening (HTS). This strategy utilizes immense computational power to screen the properties of thousands of virtual MOF structures rapidly, effectively filtering the vast chemical space down to a manageable number of promising candidates. Computational software can generate large virtual libraries of MOFs by illuminating known or hypothetical building blocks in a combinatorial way. Algorithms then predict key properties, such as surface area, pore volume, and gas adsorption capacity, for these virtual frameworks without physical synthesis. By identifying MOFs that meet prespecified performance criteria for applications like gas storage or separation, HTS provides a very effective shortcut, guiding experimentalists to the most promising synthetic targets and greatly accelerating the discovery process [150]

Complementing HTS, the integration of machine learning (ML) techniques has added another degree of sophistication to MOF optimization. ML algorithms are trained using existing experimental and computational data to discover intricate relationships between a MOF's composition, structure, and performance. This allows for the creation of predictive models that can forecast properties like ionic conductivity or catalytic activity for new MOFs before they are actually synthesized. More ambitiously, an inverse design method employs these models to suggest MOF structures that would possess a desired set of target properties, effectively reversing the typical design process. ML can also optimize synthesis conditions like temperature and reactant ratios, reducing the number of experimental cycles required to

achieve a desired material property and offering further insight into the underlying structure-property relationships [151].

Aside from predictive modeling and high-throughput screening, atomistic-level computational methods provide valuable insights into the underlying mechanisms of MOF behavior. Molecular Dynamics (MD) simulations, for instance, mimic the time-evolution of atoms to examine dynamic processes. In energy storage applications, MD can reveal the kinetics of ion transport within MOF pores, identifying bottlenecks and limitations accountable for resistance. It is also capable of modeling the adsorption and diffusion of gases or ions, giving a microscopic view of host-guest interactions and informing the design of materials with engineered transport pathways. In combination, Density Functional Theory (DFT) calculations, a quantum mechanical method, are used to examine the electronic structure of MOFs. DFT can predict electronic conductivity pathways, elucidate redox mechanisms underlying pseudocapacitive behavior, and even calculate the binding energies of guest molecules to the MOF framework with precision. This allows for accurate defect engineering and rational material design with enhanced electronic or catalytic properties.

Overall, the synergy between computational and AI-based methodologies has become an indispensable force in modern MOF research. This synergy allows efficient exploration of a large chemical space, makes accurate predictions of material properties, and provides atomic-level insights into complex phenomena that are often difficult to study experimentally. The ability to screen, optimize, and interpret MOFs at a computational level with high efficiency marks a paradigm shift from a purely empirical to a rational, data-driven design strategy. This transition is necessary in order to overcome persistent bottlenecks and unlock the full potential of MOFs to address pressing global challenges in areas such as energy storage and environmental sustainability.

5. Current Challenges and Future Perspectives

Despite the immense potential of MOFs, several issues must be addressed before they can see widespread practical use in energy storage. One of the most significant shortcomings of pure MOFs is low electronic conductivity and poor structural stability, potentially leading to degradation during repeated charge and discharge cycling. The article illustrates that synthesis methods produce the materials in small amounts with long reaction times, which presents a hindrance to large-scale industrial production. For instance, the solvothermal method, while convenient for producing high-quality crystals, is not easily scaled up. Also, the complex mechanisms for some synthetic routes, like mechanochemical methods, are not well understood yet, and controlled synthesis is challenging.

To overcome these challenges, future research will be focused on several key areas. MOF-derived composites and hybrid structures will be a priority. As the manuscript highlights, pyrolysis of MOFs to create carbon-based derivatives can significantly enhance their electrical conductivity and provide a protective framework to mitigate volume expansion during cycling. Integration of MOFs into highly conductive systems, i.e., graphene or conductive polymers, has also been highly successful in boosting performance in supercapacitors. The rational design of multi-component MOF-derived materials, as in the case of the hetero-trimetallic electrodes described, offers a pathway to synergy that boosts overall electrochemical performance.

A second critical future direction is the utilization of computational and AI-based approaches. These methodologies can substantially accelerate the discovery and optimization of MOFs with target, specific properties by predicting ideal metal-ligand combinations and framework topologies without tedious laboratory experimentation. This predictive ability can allow researchers to bypass time-consuming trial-and-error synthesis, thus accelerating the development of next-generation MOFs. Finally, continued efforts will be needed to develop scalable, green synthesis methods to make MOFs more commercially viable.

6. Conclusion

In summary, Metal-Organic Frameworks have emerged as an extremely promising group of materials in addressing the global need for high-performance energy storage. Their unique marriage of ultrahigh porosity, gigantic surface area, and exceptional structural tunability allows for remarkable manipulation of their properties, thus making them an appealing alternative to conventional materials. As described in this review, MOFs and corresponding composite materials have demonstrated exceptional performance in a wide range of applications from high-performance electrodes of batteries and supercapacitors to effective hydrogen storage. In spite of continued challenges in terms of electronic conductivity, structural stability, and scalability, continued advancement of MOF-derived hybrid materials and integration of computational design mark a new era of innovation. The future path for MOFs in energy storage is

not merely one of incremental improvement, but of a transformative impact that can change fundamentally how we store and utilize clean energy.

Compliance with ethical standards

Disclosure of conflict of interest

No conflict of interest to be disclosed.

References

[1] Adewumi, A., et al., Sustainable energy solutions and climate change: A policy review of emerging trends and global responses. World Journal of Advanced Research and Reviews, 2024. 21(2): p. 408-420.

[2] Qamruzzaman, M. and S. Karim, Unveiling the synergy: green finance, technological innovation, green energy, and carbon neutrality. Plos one, 2024. 19(10): p. e0308170.

[3] Periasamy, P. and Y.K. Mohanta, Global energy crisis: need for energy conversion and storage, in Green Nanomaterials in Energy Conversion and Storage Applications. 2024, Apple Academic Press. p. 45-73.

[4] Saleh, H.M. and A.I. Hassan, The challenges of sustainable energy transition: A focus on renewable energy. Applied Chemical Engineering, 2024. 7(2): p. 2084.

[5] Liang, Z., et al., Pristine metal–organic frameworks and their composites for energy storage and conversion. Advanced Materials, 2018. 30(37): p. 1702891.

[6] Zhang, H., et al., Metal-organic-framework-based materials as platforms for renewable energy and environmental applications. Joule, 2017. 1(1): p. 77-107.

[7] He, B., et al., Freestanding metal–organic frameworks and their derivatives: an emerging platform for electrochemical energy storage and conversion. Chemical reviews, 2022. 122(11): p. 10087-10125.

[8] Fonseca, J., et al., Metal–organic frameworks (MOFs) beyond crystallinity: amorphous MOFs, MOF liquids and MOF glasses. Journal of Materials Chemistry A, 2021. 9(17): p. 10562-10611.

[9] Cai, G., et al., Metal–organic framework-based hierarchically porous materials: synthesis and applications. Chemical Reviews, 2021. 121(20): p. 12278-12326.

[10] Wen, Y., X. Wu, and Q.L. Zhu, The Structures of Metal–Organic Frameworks. Advanced Structural Chemistry: Tailor Made, Properties and Applications of Inorganic Materials, 2021. 2: p. 342-389.

[11] Robson, R., The historical development of the concepts underlying the design and construction of targeted coordination polymers/MOFs: a personal account. The Chemical Record, 2024. 24(5): p. e202400038.

[12] Öhrström, L. and F.M.A. Noa, Metal-organic frameworks. Vol. 5. 2021: American Chemical Society.

[13] Sandhu, Z.A., et al., Metal–organic frameworks for next-generation energy storage devices; a systematic review. Materials Advances, 2024. 5(1): p. 30-50.

[14] Wang, W., et al., Metal-organic-framework-based materials as platforms for energy applications. Chem, 2024. 10(1): p. 86-133.

[15] Gangu, K.K., S. Maddila, and S.B. Jonnalagadda, The pioneering role of metal–organic framework-5 in ever-growing contemporary applications–a review. RSC advances, 2022. 12(22): p. 14282-14298.

[16] Kong, L., et al., Electrochemically active sites inside crystalline porous materials for energy storage and conversion. Chemical Society Reviews, 2020. 49(8): p. 2378-2407.

[17] Saha, R. and C.J.G. García, extrinsically conducting MOFs: guest-promoted enhancement of electrical conductivity, thin film fabrication and applications. Chemical Society Reviews, 2024.

[18] Laeim, H., et al., Porosity tunable metal-organic framework (MOF)-based composites for energy storage applications: recent progress. Polymers, 2025. 17(2): p. 130.

[19] Hassan, Z., et al., Assembly of molecular building blocks into integrated complex functional molecular systems: structuring matter made to order. Advanced Functional Materials, 2020. 30(26): p. 1907625.

[20] Liu, Y., et al., Design of complex nanomaterials for energy storage: past success and future opportunity. Accounts of chemical research, 2017. 50(12): p. 2895-2905.

[21] Chen, W., L. Du, and C. Wu, Hydrothermal synthesis of MOFs, in Metal-organic frameworks for biomedical applications. 2020, Elsevier. p. 141-157.

[22] Ghoorchian, A., et al., Electrochemical synthesis of MOFs, in Metal-organic frameworks for biomedical applications. 2020, Elsevier. p. 177-195.

[23] Tanaka, S., Mechanochemical synthesis of MOFs. Metal-Organic Frameworks for Biomedical Applications, 2020: p. 197-222.

[24] Nguyen, V.H., et al., Facile synthesis of bismuth (III) based metal-organic framework with difference ligands using microwave irradiation method. Chemical Engineering Research and Design, 2022. 177: p. 321-330.

[25] Zheng, S.Q., et al., Solvothermal synthesis of nanostructured nickel-based metal–organic frameworks (Ni-MOFs) with enhanced electrochemical performance for symmetric supercapacitors. Journal of Materials Science, 2023. 58(29): p. 11894-11913.

[26] Mubeen, M., et al., Synthesis Strategies of. Multifunctional Coordination Materials for Green Energy Technologies. 37.

[27] Lin, H., et al., Postsynthetic modification of metal– organic frameworks for photocatalytic applications. Small Structures, 2022. 3(5): p. 2100176.

[28] Zhang, X., et al., Metal–organic frameworks (MOFs) and MOF-derived materials for energy storage and conversion. Electrochemical Energy Reviews, 2019. 2(1): p. 29-104.

[29] Banerjee, R., et al., High-throughput synthesis of zeolitic imidazolate frameworks and application to CO2 capture. Science, 2008. 319(5865): p. 939-943.

[30] McKinstry, C., et al., Scalable continuous solvothermal synthesis of metal organic framework (MOF-5) crystals. Chemical Engineering Journal, 2016. 285: p. 718-725.

[31] Cho, H.-Y., et al., CO2 adsorption and catalytic application of Co-MOF-74 synthesized by microwave heating. Catalysis Today, 2012. 185(1): p. 35-40.

[32] Lalawmpuia, R., M. Lalhruaitluangi, and D. Tiwari, Metal organic framework (MOF): Synthesis and fabrication for the application of electrochemical sensing. Environmental Engineering Research, 2024. 29(5).

[33] Martinez Joaristi, A., et al., Electrochemical synthesis of some archetypical Zn2+, Cu2+, and Al3+ metal organic frameworks. Crystal Growth and Design, 2012. 12(7): p. 3489-3498.

[34] Klimakow, M., et al., Mechanochemical synthesis of metal– organic frameworks: a fast and facile approach toward quantitative yields and high specific surface areas. Chemistry of Materials, 2010. 22(18): p. 5216-5221.

[35] Mangaiyarkkarasi, J., Nanostructural Innovations: Powering the Future of Energy Storage, in Design, Fabrication, and Significance of Advanced Nanostructured Materials. 2025, IGI Global. p. 51-74.

[36] Li, D., et al., Advances and applications of metal-organic frameworks (MOFs) in emerging technologies: a comprehensive review. Global Challenges, 2024. 8(2): p. 2300244.

[37] Wu, H.B. and X.W. Lou, Metal-organic frameworks and their derived materials for electrochemical energy storage and conversion: Promises and challenges. Science Advances, 2017. 3(12): p. eaap9252.

[38] Du, R., et al., Porosity engineering of MOF-based materials for electrochemical energy storage. Advanced Energy Materials, 2021. 11(20): p. 2100154.

[39] Shanmugam, M., et al., Metal–organic frameworks (MOFs) for energy production and gaseous fuel and electrochemical energy storage applications. Physical Chemistry Chemical Physics, 2023. 25(44): p. 30116-30144.

[40] Wang, W., et al., Multi-metallic MOF based composites for environmental applications: synergizing metal centers and interactions. Nanoscale Horizons, 2024. 9(9): p. 1432-1474.

[41] Argirusis, C., et al., Advances in Metal-Organic Frameworks (MOFs) for Rechargeable Batteries and Fuel Cells. Batteries, 2025. 11(5): p. 192.

[42] Argirusis, C., et al., Recent Advances in the Application of MOFs in Supercapacitors. Batteries, 2025. 11(5): p. 181.

[43] Geng, P., et al., MIL-96-Al for Li–S batteries: shape or size? Advanced Materials, 2022. 34(4): p. 2107836.

[44] Zhang, Q., et al., All-metal-organic framework-derived battery materials on carbon nanotube fibers for wearable energy-storage device. Advanced Science, 2018. 5(12): p. 1801462.

[45] Dubal, D.P., et al., Metal–organic framework (MOF) derived electrodes with robust and fast lithium storage for Li-ion hybrid capacitors. Advanced Functional Materials, 2019. 29(19): p. 1900532.

[46] Li, M., et al., Metal–organic framework-based separators for enhancing Li–S battery stability: mechanism of mitigating polysulfide diffusion. ACS Energy Letters, 2017. 2(10): p. 2362-2367.

[47] Gao, X., et al., COFs for batteries and supercapacitors. Electrochem Energy Rev, 2020. 3(1): p. 81-126.

[48] Fang, G., et al., MOFs nanosheets derived porous metal oxide-coated three-dimensional substrates for lithium-ion battery applications. Nano Energy, 2016. 26: p. 57-65.

[49] Sun, J.-K. and Q. Xu, Functional materials derived from open framework templates/precursors: synthesis and applications. Energy and Environmental Science, 2014. 7(7): p. 2071-2100.

[50] Wang, Y., et al., Excellent performance in lithium-ion battery anodes: rational synthesis of Co (CO3) 0.5 (OH) 0.11 H2O nanobelt array and its conversion into mesoporous and single-crystal Co3O4. ACS nano, 2010. 4(3): p. 1425-1432.

[51] Kong, D., et al., Three-dimensional Co3O4@ MnO2 hierarchical nanoneedle arrays: morphology control and electrochemical energy storage. Advanced Functional Materials, 2014. 24(24): p. 3815-3826.

[52] Hu, H., et al., unusual formation of CoSe@ carbon nanoboxes, which have an inhomogeneous shell, for efficient lithium storage. Angewandte chemie international edition, 2016. 55(33): p. 9514-9518.

[53] Zhang, Z., H. Yoshikawa, and K. Awaga, Monitoring the solid-state electrochemistry of Cu (2, 7-AQDC)(AQDC= anthraquinone dicarboxylate) in a lithium battery: coexistence of metal and ligand redox activities in a metal–organic framework. Journal of the American Chemical Society, 2014. 136(46): p. 16112-16115.

[54] Peng, Z., et al., Triphenylamine-based metal–organic frameworks as cathode materials in lithium-ion batteries with coexistence of redox active sites, high working voltage, and high rate stability. ACS applied materials and interfaces, 2016. 8(23): p. 14578-14585.

[55] Luo, X., et al., Trimetallic metal–organic frameworks and derived materials for environmental remediation and electrochemical energy storage and conversion. Coordination Chemistry Reviews, 2022. 461: p. 214505.

[56] Lin, X., et al., Copper nanowires and copper foam multifunctional bridges in zeolitic imidazolate framework–derived anode material for superior lithium storage. Journal of colloid and interface science, 2020. 565: p. 156-166.

[57] Yuan, C., et al., Mixed transition-metal oxides: design, synthesis, and energy-related applications. Angewandte Chemie International Edition, 2014. 53(6): p. 1488-1504.

[58] Guo, L., et al., Pineapple-shaped ZnCo 2 O 4 microspheres as anode materials for lithium ion batteries with prominent rate performance. Journal of Materials Chemistry A, 2015. 3(16): p. 8683-8692.

[59] Lin, J., et al., Trimetallic MOF-derived Cu0. 39Zn0. 14Co2. 47O4–CuO interwoven with carbon nanotubes on copper foam for superior lithium storage with boosted kinetics. ACS Sustainable Chemistry and Engineering, 2019. 7(18): p. 15684-15695.

[60] Njema, G.G., R.B.O. Ouma, and J.K. Kibet, A review on the recent advances in battery development and energy storage technologies. Journal of renewable energy, 2024. 2024(1): p. 2329261.

[61] Dong, S., et al., ZnS-Sb2S3@ C core-double shell polyhedron structure derived from metal–organic framework as anodes for high performance sodium ion batteries. Acs Nano, 2017. 11(6): p. 6474-6482.

[62] Yue, M., et al., Carbon-Coated MOF-Derived Porous SnPS3 Core–Shell Structure as Superior Anode for Sodium-Ion Batteries. Small, 2024. 20(47): p. 2405262.

[63] Tian, S., et al., Capacitive deionization with nitrogen-doped highly ordered mesoporous carbon electrodes. Chemical Engineering Journal, 2020. 380: p. 122514.

[64] Wang, L., et al., General metal–organic framework-derived strategy to synthesize yolk-shell carbon-encapsulated nickelic spheres for sodium-ion batteries. Journal of Colloid and Interface Science, 2022. 613: p. 23-34.

[65] Ren, J., et al., Recent progress on MOF-derived carbon materials for energy storage. Carbon Energy, 2020. 2(2): p. 176-202.

[66] Bucur, C.B., et al., Inorganic–organic layer by layer hybrid membranes for lithium–sulfur batteries. Energy and Environmental Science, 2017. 10(4): p. 905-911.

[67] Zhao, Z., et al., Graphene-wrapped chromium-MOF (MIL-101)/sulfur composite for performance improvement of high-rate rechargeable Li–S batteries. Journal of materials chemistry A, 2014. 2(33): p. 13509-13512.

[68] Yang, J., et al., A MIL-47 (V) derived hierarchical lasagna-structured V 2 O 3@ C hollow microcuboid as an efficient sulfur host for high-performance lithium–sulfur batteries. Nanoscale, 2020. 12(7): p. 4552-4561.

[69] Chen, D., et al., Two-dimensional square metal organic framework as promising cathode material for lithium-sulfur battery with high theoretical energy density. Journal of Colloid and Interface Science, 2022. 613: p. 435-446.

[70] Li, W., et al., Rational design and general synthesis of multimetallic metal–organic framework nano-octahedra for enhanced Li–S battery. Advanced Materials, 2021. 33(45): p. 2105163.

[71] Hong, X.-J., et al., Confinement of polysulfides within bi-functional metal–organic frameworks for high performance lithium–sulfur batteries. Nanoscale, 2018. 10(6): p. 2774-2780.

[72] Bai, L., et al., Refined sulfur nanoparticles immobilized in metal–organic polyhedron as stable cathodes for Li–S battery. ACS Applied Materials and Interfaces, 2016. 8(23): p. 14328-14333.

[73] Demir-Cakan, R., et al., Cathode composites for Li–S batteries via the use of oxygenated porous architectures. Journal of the American Chemical Society, 2011. 133(40): p. 16154-16160.

[74] Wang, Z., et al., Sulfur encapsulated ZIF-8 as cathode material for lithium–sulfur battery with improved cyclability. Microporous and mesoporous materials, 2014. 185: p. 92-96.

[75] Zhou, J., et al., Rational design of a metal–organic framework host for sulfur storage in fast, long-cycle Li–S batteries. Energy and Environmental Science, 2014. 7(8): p. 2715-2724.

[76] Bao, W., et al., Confine sulfur in mesoporous metal–organic framework@ reduced graphene oxide for lithium sulfur battery. Journal of Alloys and Compounds, 2014. 582: p. 334-340.

[77] Park, J.H., et al., Encapsulation of redox polysulphides via chemical interaction with nitrogen atoms in the organic linkers of metal-organic framework nanocrystals. Scientific reports, 2016. 6(1): p. 25555.

[78] Zhou, J., et al., The impact of the particle size of a metal–organic framework for sulfur storage in Li–S batteries. Journal of Materials Chemistry A, 2015. 3(16): p. 8272-8275.

[79] Bhambri, H. and S.K. Mandal, Impact of Conformational Isomerism in Two Zn-MOFs on the Multimedia Incarceration of Iodine: In-Depth Experimental and Computational Assessments. ACS Applied Energy Materials, 2023. 6(24): p. 12307-12317.

[80] Cao, J., et al., Effect of external direct current electric field on the inhibition behavior of Zn-MOFs for Cu in 0.5 mol/L NaCl solution. Colloids and Surfaces A: Physicochemical and Engineering Aspects, 2022. 632: p. 127751.

[81] Cao, X., et al., Hybrid micro-/nano-structures derived from metal–organic frameworks: preparation and applications in energy storage and conversion. Chemical Society Reviews, 2017. 46(10): p. 2660-2677.

[82] Cao, Z., et al., Metal–organic framework materials for electrochemical supercapacitors. Nano-micro letters, 2022. 14(1): p. 181.

[83] Wei, J., et al., Advanced electrolytes for high-performance aqueous zinc-ion batteries. Chemical Society Reviews, 2024.

[84] Hu, R.Y., et al., Preparation and electrochemical properties of bimetallic carbide Fe3Mo3C/Mo2C@ carbon nanotubes as negative electrode material for supercapacitor. Journal of Energy Storage, 2023. 72: p. 108656.

[85] Hu, X., et al., A signal-on electrochemiluminescence sensor for clenbuterol detection based on zinc-based metal-organic framework–reduced graphene oxide–CdTe quantum dot hybrids. Analytical and Bioanalytical Chemistry, 2018. 410(30): p. 7881-7890.

[86] Kumar, Y.A., et al., 2D MXene-based supercapacitors: A promising path towards high-performance energy storage. Journal of Energy Storage, 2023. 72: p. 108433.

[87] Li, S., et al., Transition metal-based bimetallic MOFs and MOF-derived catalysts for electrochemical oxygen evolution reaction. Energy and Environmental Science, 2021. 14(4): p. 1897-1927.

[88] Xu, Y., et al., Nickel Nanoparticles Encapsulated in Few-Layer Nitrogen-Doped Graphene Derived from Metal-Organic Frameworks as Efficient Bifunctional Electrocatalysts for Overall Water Splitting. Advanced Materials (Deerfield Beach, Fla.), 2017. 29(11).

[89] He, B., et al., Self-sacrificed synthesis of conductive vanadium-based metal–organic framework nanowire-bundle arrays as binder-free cathodes for high-rate and high-energy-density wearable Zn-ion batteries. Nano Energy, 2019. 64: p. 103935.

[90] Kumar, Y.A., et al., Solidifying the future: Metal-organic frameworks in zinc battery development. Journal of Energy Storage, 2024. 97: p. 112826.

[91] Yin, C., et al., Coordinately unsaturated manganese-based metal–organic frameworks as a high-performance cathode for aqueous zinc-ion batteries. ACS Applied Materials and Interfaces, 2021. 13(30): p. 35837-35847.

[92] Alzard, R.H., et al., Structural analysis and photocatalytic activities of bismuth-lanthanide oxide perovskites. Journal of Solid-State Chemistry, 2024. 329: p. 124359.

[93] Raja, A., et al., A quintuple-layered binary chalcogenide Sb2Te3 single crystal and its transport properties for thermoelectric applications. ACS omega, 2022. 7(32): p. 27798-27803.

[94] Fu, Y., et al., High-performance reversible aqueous Zn-ion battery based on porous MnOx nanorods coated by MOF-derived N-doped carbon. Advanced Energy Materials, 2018. 8(26): p. 1801445.

[95] Nam, K.W., et al., Conductive 2D metal-organic framework for high-performance cathodes in aqueous rechargeable zinc batteries. Nature communications, 2019. 10(1): p. 4948.

[96] Zhang, S., et al., Vanadium hexacyanoferrate as a high-capacity and high-voltage cathode for aqueous rechargeable zinc ion batteries. Nanomaterials, 2022. 12(23): p. 4268.

[97] Gou, L., et al., Mn 2 O 3/Al 2 O 3 cathode material derived from a metal–organic framework with enhanced cycling performance for aqueous zinc-ion batteries. Dalton Transactions, 2020. 49(3): p. 711-718.

[98] Dhilip, M., et al., A novel double perovskite oxide Sm2CoFeO6 phosphor for orange LEDs: structural, magnetic and luminescence properties. Applied Physics A, 2022. 128(4): p. 324.

[99] Ma, L., et al., Achieving high-voltage and high-capacity aqueous rechargeable zinc ion battery by incorporating two-species redox reaction. Advanced Energy Materials, 2019. 9(45): p. 1902446.

[100] Ni, G., et al., Potassium manganese hexacyanoferrate with improved lifespan in Zn (CF 3 SO 3) 2 electrolyte for aqueous zinc-ion batteries. Sustainable Energy and Fuels, 2022. 6(5): p. 1353-1361.

[101] Zeeshan, M. and M. Shahid, State of the art developments and prospects of metal–organic frameworks for energy applications. Dalton Transactions, 2022. 51(5): p. 1675-1723.

[102] Barik, R. and P.P. Ingole, Challenges and prospects of metal sulfide materials for supercapacitors. Current Opinion in Electrochemistry, 2020. 21: p. 327-334.

[103] Choudhary, R.B., S. Ansari, and B. Purty, Robust electrochemical performance of polypyrrole (PPy) and polyindole (PIn) based hybrid electrode materials for supercapacitor application: A review. Journal of Energy Storage, 2020. 29: p. 101302.

[104] Iro, Z.S., C. Subramani, and S. Dash, A brief review on electrode materials for supercapacitor. International Journal of Electrochemical Science, 2016. 11(12): p. 10628-10643.

[105] Wang, G., L. Zhang, and J. Zhang, A review of electrode materials for electrochemical supercapacitors. Chemical Society Reviews, 2012. 41(2): p. 797-828.

[106] Pang, J., et al., Facile and sustainable synthesis of sodium lignosulfonate derived hierarchical porous carbons for supercapacitors with high volumetric energy densities. Green chemistry, 2017. 19(16): p. 3916-3926.

[107] Kandalkar, S., et al., Chemical synthesis of cobalt oxide thin film electrode for supercapacitor application. Synthetic Metals, 2010. 160(11-12): p. 1299-1302.

[108] Sanati, S., et al., Metal–organic framework derived bimetallic materials for electrochemical energy storage. Angewandte Chemie International Edition, 2021. 60(20): p. 11048-11067.

[109] Pershaanaa, M., et al., Every bite of Supercap: A brief review on construction and enhancement of supercapacitor. Journal of Energy Storage, 2022. 50: p. 104599.

[110] Lakra, R., et al., A mini-review: Graphene based composites for supercapacitor application. Inorganic Chemistry Communications, 2021. 133: p. 108929.

[111] Zhao, Y., et al., Hierarchical NiCo2S4@ CoMoO4 core-shell heterostructures nanowire arrays as advanced electrodes for flexible all-solid-state asymmetric supercapacitors. Applied Surface Science, 2018. 453: p. 73-82.

[112] Attia, S.Y., et al., Supercapacitor electrode materials: addressing challenges in mechanism and charge storage. Reviews in Inorganic Chemistry, 2022. 42(1): p. 53-88.

[113] Augustyn, V., P. Simon, and B. Dunn, Pseudocapacitive oxide materials for high-rate electrochemical energy storage. Energy and Environmental Science, 2014. 7(5): p. 1597-1614.

[114] Qiu, T., et al., Metal–organic framework-based materials for energy conversion and storage. ACS Energy Letters, 2020. 5(2): p. 520-532.

[115] Ren, X., et al., Two-dimensional MOF and COF nanosheets for next-generation optoelectronic applications. Coordination Chemistry Reviews, 2021. 435: p. 213781.

[116] Ramachandran, R., et al., Morphology-dependent electrochemical properties of cobalt-based metal organic frameworks for supercapacitor electrode materials. Electrochimica Acta, 2018. 267: p. 170-180.

[117] Li, Y., et al., MOF-derived metal oxide composites for advanced electrochemical energy storage. Small, 2018. 14(25): p. 1704435.

[118] Srinivasan, R., et al., Enhanced electrochemical behaviour of Co-MOF/PANI composite electrode for supercapacitors. Inorganica chimica acta, 2020. 502: p. 119393.

[119] Wang, X., et al., Solvothermal synthesis of flower-string-like NiCo-MOF/MWCNT composites as a high-performance supercapacitor electrode material. Journal of Solid-State Chemistry, 2019. 277: p. 575-586.

[120] Yuan, J., et al., Controlled synthesis of flower-like hierarchical NiCo-layered double hydroxide integrated with metal–organic framework-derived Co@ C for supercapacitors. ACS Applied Materials and Interfaces, 2023. 15(30): p. 36143-36153.

[121] Panda, P., et al., Ultrathin Ni–Co bimetallic metal–organic framework nanobelts for high-performance energy storage. ACS Applied Nano Materials, 2023. 6(17): p. 15916-15924.

[122] Acharya, D., et al., In situ transmogrification of nanoarchitectured Fe-MOFs decorated porous carbon nanofibers into efficient positrode for asymmetric supercapacitor application. Journal of Energy Storage, 2023. 63: p. 106992.

[123] Sun, P., et al., Bimetallic MOF-derived (CuCo) Se nanoparticles embedded in nitrogen-doped carbon framework with boosted electrochemical performance for hybrid supercapacitor. Materials Research Bulletin, 2021. 137: p. 111196.

[124] Xu, J., et al., NiFe 2 O 4 quantum dots anchored on flower-like Ni-MOF with enhanced electrochemical performance for supercapacitors. Journal of Materials Chemistry C, 2023. 11(44): p. 15624-15637.

[125] Choi, K.M., et al., Supercapacitors of nanocrystalline metal–organic frameworks. ACS nano, 2014. 8(7): p. 7451-7457.

[126] Sheberla, D., et al., Conductive MOF electrodes for stable supercapacitors with high areal capacitance. Nature materials, 2017. 16(2): p. 220-224.

[127] Gu, M., et al., Morphology control of nanoscale metal-organic frameworks for high-performance supercapacitors. Electrochimica Acta, 2020. 343: p. 135617.

[128] Wu, M.K., et al., MOF–derived hollow double–shelled NiO nanospheres for high–performance supercapacitors. Journal of Alloys and Compounds, 2018. 734: p. 1-8.

[129] Zhu, Z., et al., Facile synthesis of MOF-derived porous spinel zinc manganese oxide/carbon nanorods hybrid materials for supercapacitor application. Ceramics International, 2018. 44(16): p. 20163-20169.

[130] Rahmanifar, M.S., et al., A dual Ni/Co-MOF-reduced graphene oxide nanocomposite as a high-performance supercapacitor electrode material. Electrochimica Acta, 2018. 275: p. 76-86.

[131] Pan, Y., et al., Fishbone-like Ni3S2/Co3S4 integrated with nickel MOF nanosheets for hybrid supercapacitors. Applied Surface Science, 2021. 566: p. 150744.

[132] Manikandan, M., et al., Influence of hydrothermal reaction time on the supercapacitor performance of Ni-MOF nanostructures. Applied Physics A, 2021. 127(6): p. 421.

[133] Kumar, S., et al., Bifunctional rGO-NiCo2S4 MOF hybrid with high electrochemical and catalytic activity for supercapacitor and nitroarene reduction. Journal of Materials Research and Technology, 2021. 12: p. 2489-2501.

[134] Kumaraguru, S., J. Yesuraj, and S. Mohan, Reduced graphene oxide-wrapped micro-rod like Ni/Co organic-inorganic hybrid nanocomposite as an electrode material for high-performance supercapacitor. Composites Part B: Engineering, 2020. 185: p. 107767.

[135] Zhao, W., et al., MOF derived Ni-Co-S nanosheets on electrochemically activated carbon cloth via an etching/ion exchange method for wearable hybrid supercapacitors. Chemical engineering journal, 2019. 371: p. 461-469.

[136] Meng, X.-X., et al., MOF-derived NiO nanoparticles prilled by controllable explosion of perchlorate ion: excellent performances and practical applications in supercapacitors. Applied Surface Science, 2020. 507: p. 145077.

[137] Wang, J., et al., Fabrication of 3D Co-doped Ni-based MOF hierarchical micro-flowers as a high-performance electrode material for supercapacitors. Applied Surface Science, 2019. 483: p. 1158-1165.

[138] Deng, T., et al., Inverted design for high-performance supercapacitor via Co (OH) 2-derived highly oriented MOF electrodes. Advanced Energy Materials, 2018. 8(7): p. 1702294.

[139] Shi, L., et al., In situ deposition of conducting polymer on metal organic frameworks for high performance hybrid supercapacitor electrode materials. Journal of Energy Storage, 2022. 52: p. 104729.

[140] Rabani, I., et al., Hierarchical structured nano-polyhedrons of CeO2@ ZIF-8 composite for high performance supercapacitor applications. Journal of Alloys and Compounds, 2021. 875: p. 160074.

[141] Li, H., et al., porous metal-organic frameworks for gas storage and separation: Status and challenges. EnergyChem, 2019. 1(1): p. 100006.

[142] Chen, Z., et al., porous materials for hydrogen storage. Chem, 2022. 8(3): p. 693-716.

[143] Rosi, N.L., et al., Hydrogen storage in microporous metal-organic frameworks. Science, 2003. 300(5622): p. 1127-1129.

[144] Kaye, S.S., et al., Impact of preparation and handling on the hydrogen storage properties of Zn4O (1, 4-benzenedicarboxylate) 3 (MOF-5). Journal of the American Chemical Society, 2007. 129(46): p. 14176-14177.

[145] Furukawa, H., et al., Ultrahigh porosity in metal-organic frameworks. Science, 2010. 329(5990): p. 424-428.

[146] Zhang, X., et al., Optimization of the pore structures of MOFs for record high hydrogen volumetric working capacity. Advanced materials, 2020. 32(17): p. 1907995.

[147] Wang, B., et al., A microporous aluminum-based metal-organic framework for high methane, hydrogen, and carbon dioxide storage. Nano Research, 2021. 14(2): p. 507-511.

[148] Han, S.S., W.Q. Deng, and W.A. Goddard III, Improved designs of metal–organic frameworks for hydrogen storage. Angewandte Chemie, 2007. 119(33): p. 6405-6408.

[149] Ma, Q., et al., Computational design of Metal-Organic Frameworks for sustainable energy and environmental applications: Bridging theory and experiment. Materials Science and Engineering: B, 2025. 311: p. 117765.

[150] Shi, Z., et al., Machine-learning-assisted high-throughput computational screening of high-performance metal–organic frameworks. Molecular Systems Design and Engineering, 2020. 5(4): p. 725-742.

[151] Chafiq, M., A. Chaouiki, and Y.G. Ko, Targeted metal–organic framework discovery goes digital: machine learning's quest from algorithms to atom arrangements. Advanced Composites and Hybrid Materials, 2024. 7(6): p. 222.